INTERNATIONAL ATOMIC ENERGY AGENCY
UNITED NATIONS EDUCATIONAL, SCIENTIFIC AND CULTURAL ORGANIZATION
INTERNATIONAL CENTRE FOR THEORETICAL PHYSICS
I.C.T.P., P.O. BOX 586, 34100 TRIESTE, ITALY, CABLE: CENTRATOM TRIESTE

SMR.627-5

MINIWORKSHOP ON
STRONGLY CORRELATED ELECTRON SYSTEMS

15 JUNE - 10 JULY 1992

"ELECTRONIC PROPERTIES"
Part II

A. RAMIREZ
AT&T Bell Laboratories
600 Mountain Avenue
Murray Hill, NJ 07974-2070
U.S.A.

ELECTRONIC PROPERTIES

- A_6C_{60}
  - — Filled band insulator
- A_2C_{60} and A_4C_{60}
  - — Gap in Na_2 by photoemission (Gu, et al)
  - — ^{13}C NMR T_1T strong function of T
- Most A_3C_{60} metallic and superconducting
  - — ^{13}C T_1T doubles for Na_2Rb from 290K to 100K and 6X for Na_3

Variation of T_c with lattice constant

M. Schlüter et al, preprint

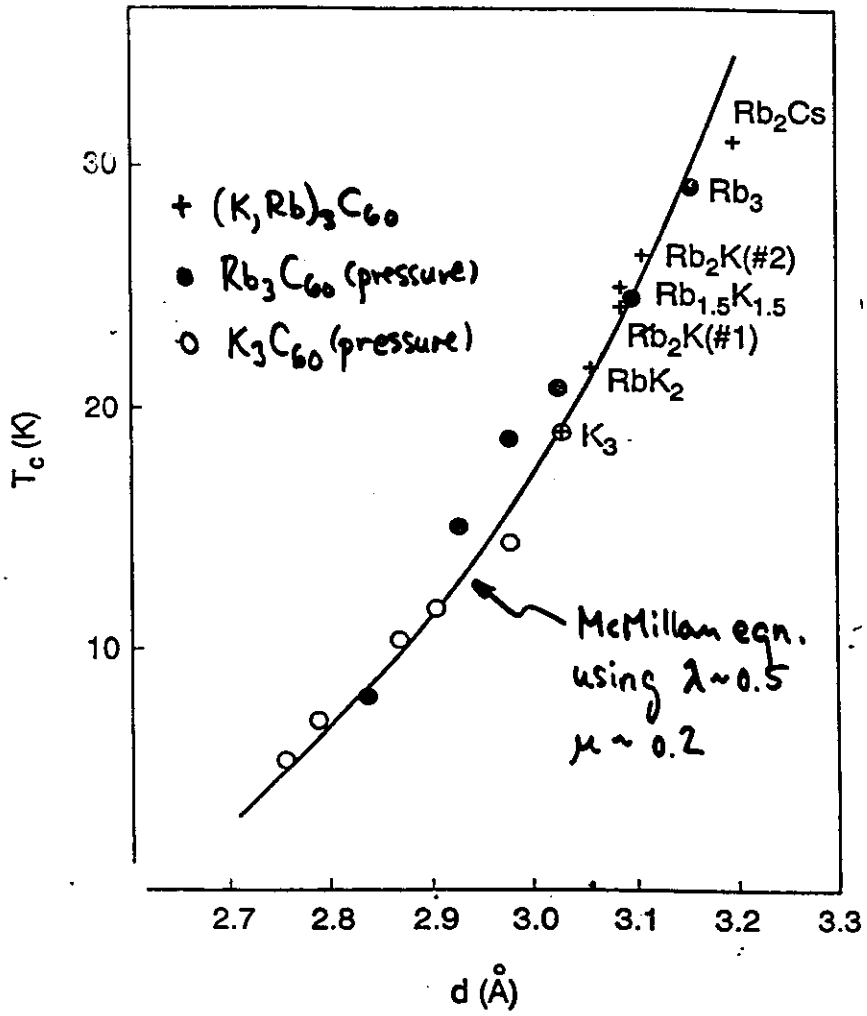

Photoemmission Spectroscopy in K_xC_{60}

C.T. Chen et al, Nature 352, 603(1991)

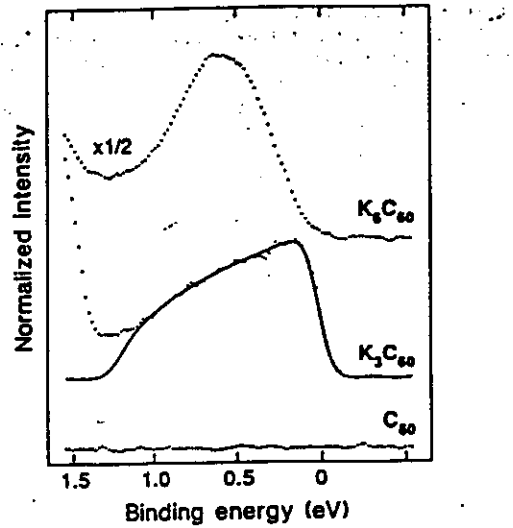

Photoemission of Metallic + Insulating Phases

Gu et al, PRB 45, 6748 (1992)

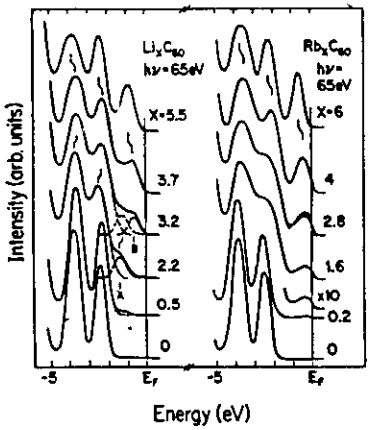

FIG. 1. Photoemission spectra for Li_xC_{60} and Rb_xC_{60} with energies referenced to the Fermi level of the spectrometer, E_F. The nonmetallic behavior of Li_xC_{60} for all x values is indicated by the lack of emission at E_F. In contrast, Rb_xC_{60} films exhibit metallic Fermi edges. Doping to A_6C_{60} produces complete filling of the LUMO-derived band and recovery to the insulating molecular-solid configuration. The dashed lines for Li_xC_{60} provide a guide to the eye for bands A and B. That for $Rb_{2.8}C_{60}$ shows the effect of enhanced experimental resolution.

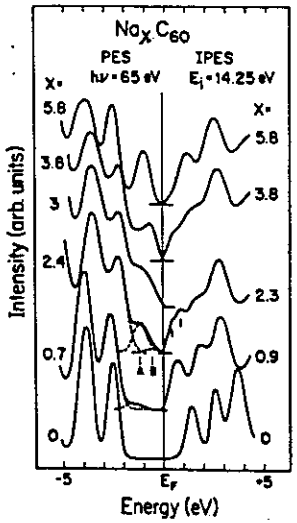

FIG. 2. Photoemission and inverse photoemission results for Na_xC_{60}, showing the evolution of the occupied and empty states near E_F. Feature A corresponds to Na_2C_{60} and feature B reflects conversion to the Na_6C_{60} phase. For $Na_{2.3}C_{60}$, splitting is evident in the leading conduction-band feature. The movement of spectral features relative to E_F reflects changes in screening with pinning of E_F at the conduction-band minimum.

Pseudo-Gap at the Fermi Level in K_3C_{60}

Takahashi et al, PRL 68, 1232 (1992)

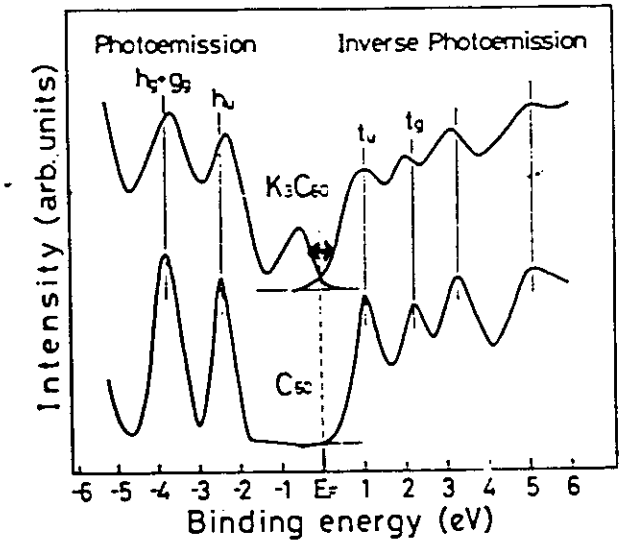

FIG. 1. Photoemission and inverse photoemission spectra of C_{60} and K_3C_{60}.

- Chen et al PRL (comment) –
  - samples not annealed
  - surface effects dominate (Raman study)
  - IPES not consistent w/ Minnesota data showing t_{1u} intersects Fermi level at $x = 3$.

Surface Effects in Photoemission

Wertheim et al., preprint

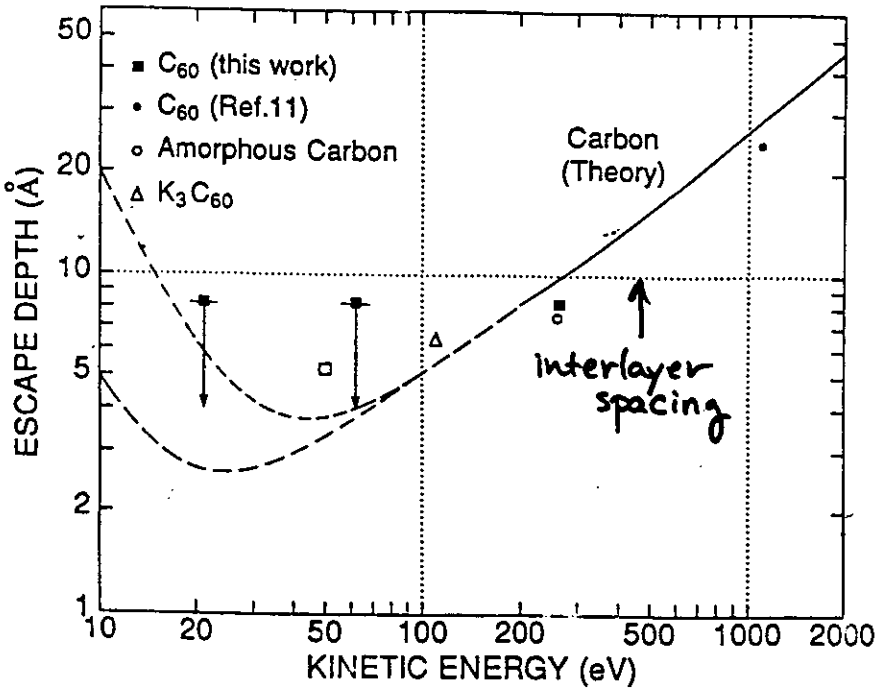

- Molecular solids pose special problem for PES
- In C_{60}, only 1st monolayer probed.

Surface effects in Photoemission

Wertheim et al., preprint

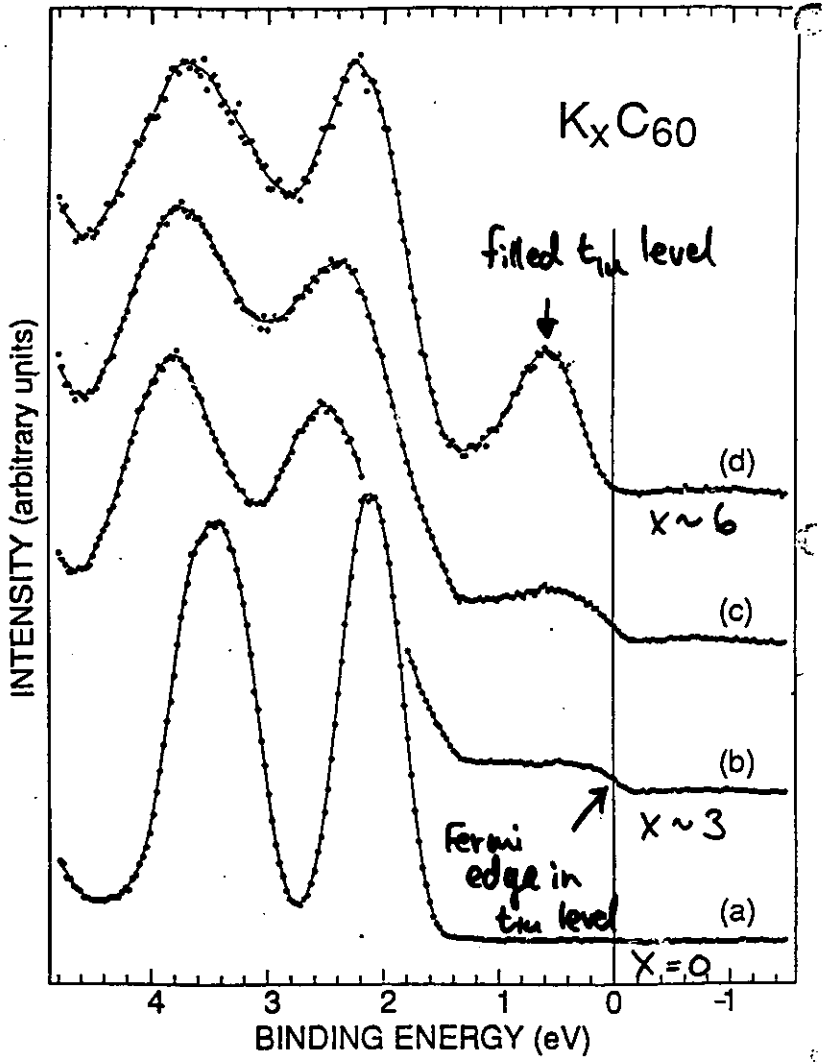

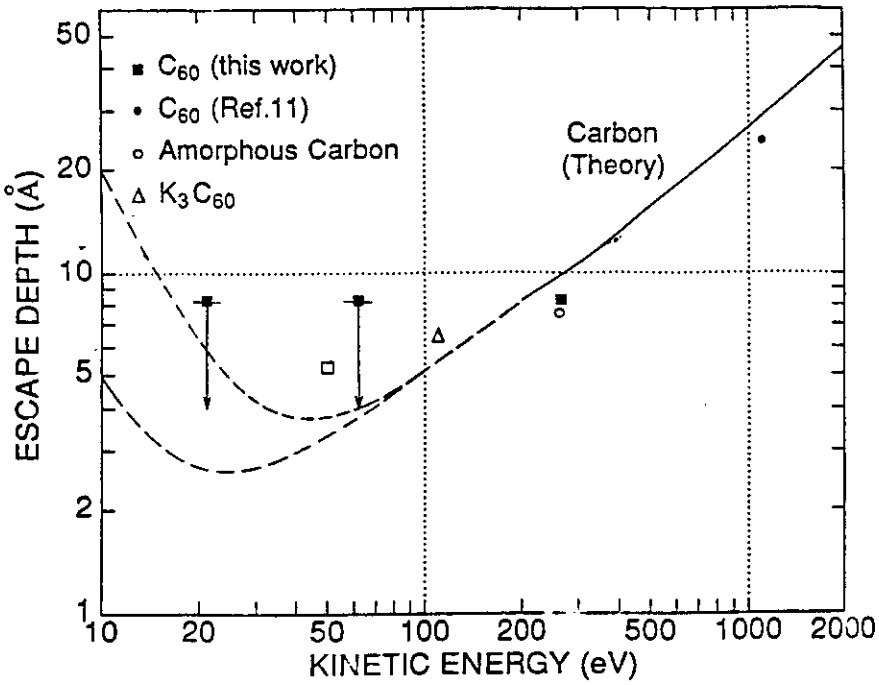

Ferromagnetism in $C_{60}(TDAE)_x$

Allemand, et al

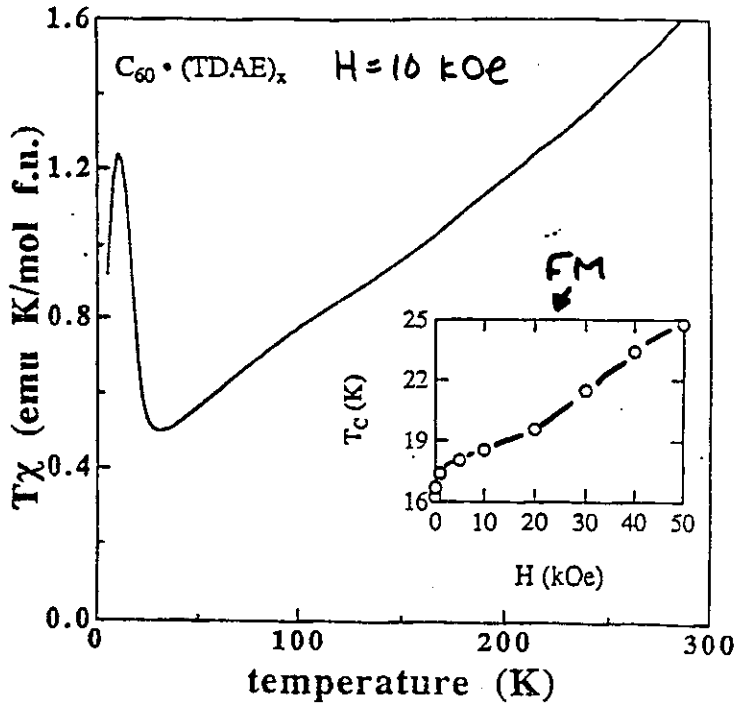

- Increasing T_c with H signals FM state.

Ferromagnetism in $C_{60}(TDAE)_x$

Allemand, Wudl, etal,

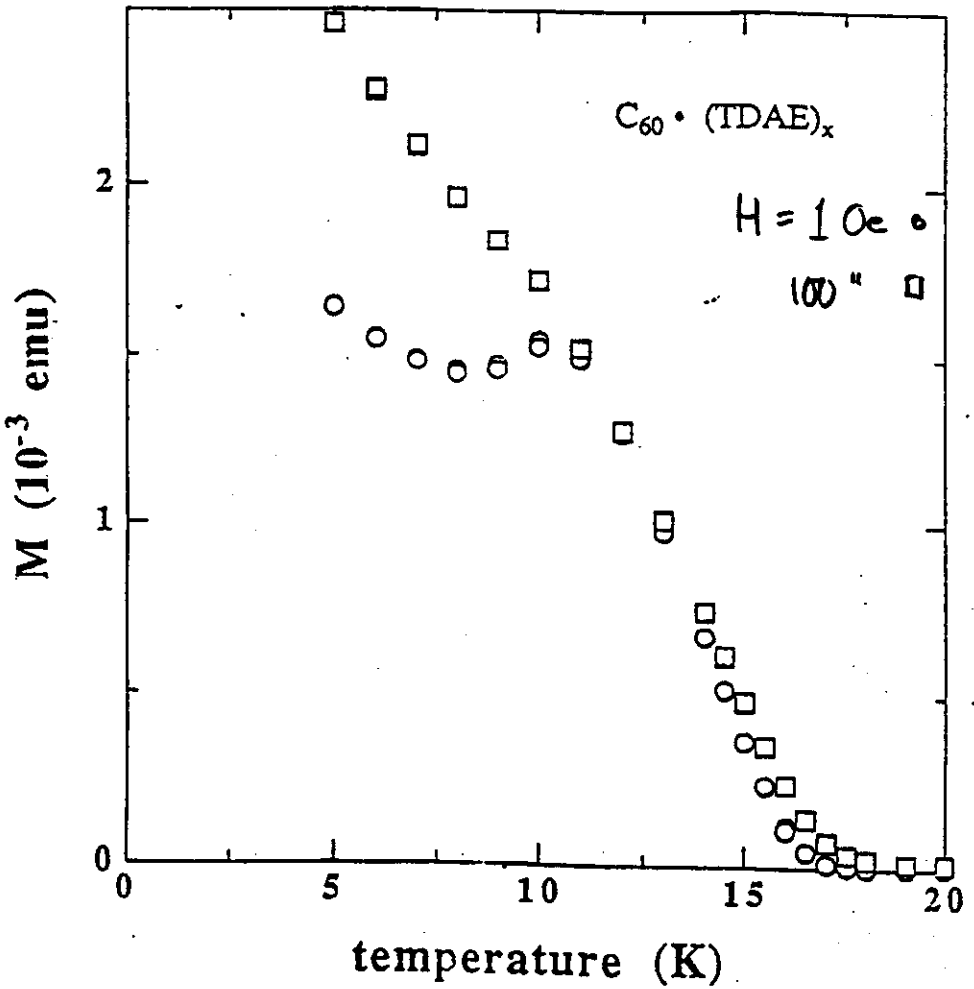

Ferromagnetism in $C_{60}(TDAE)_x$

Allemand et al.

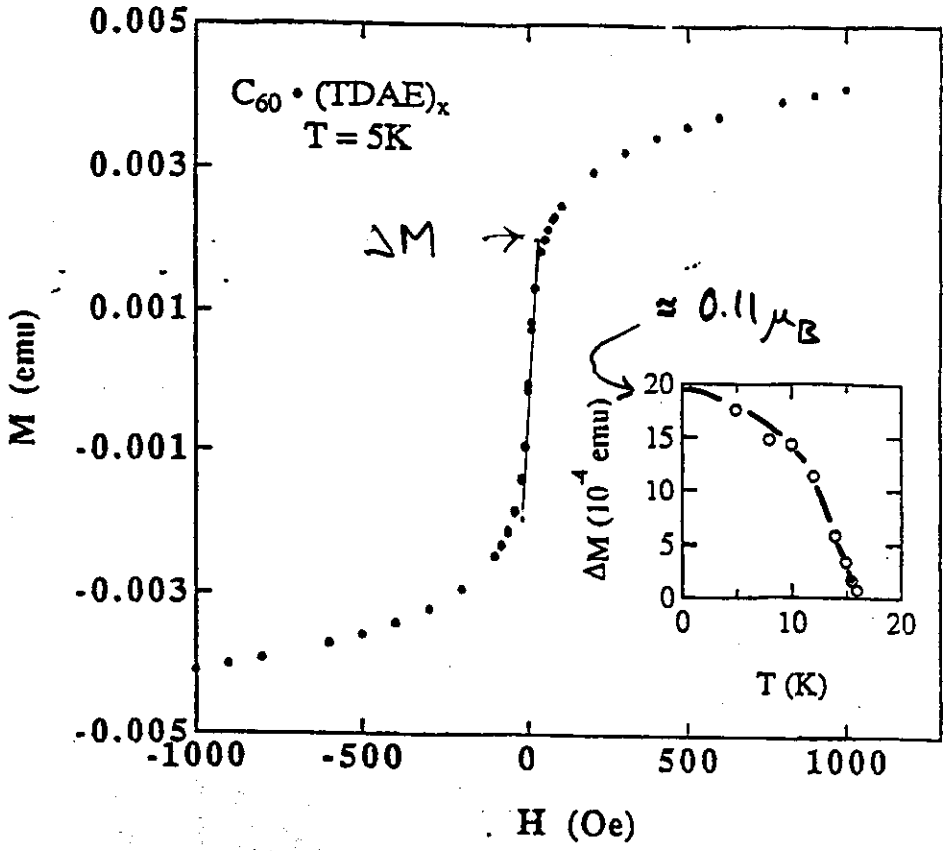

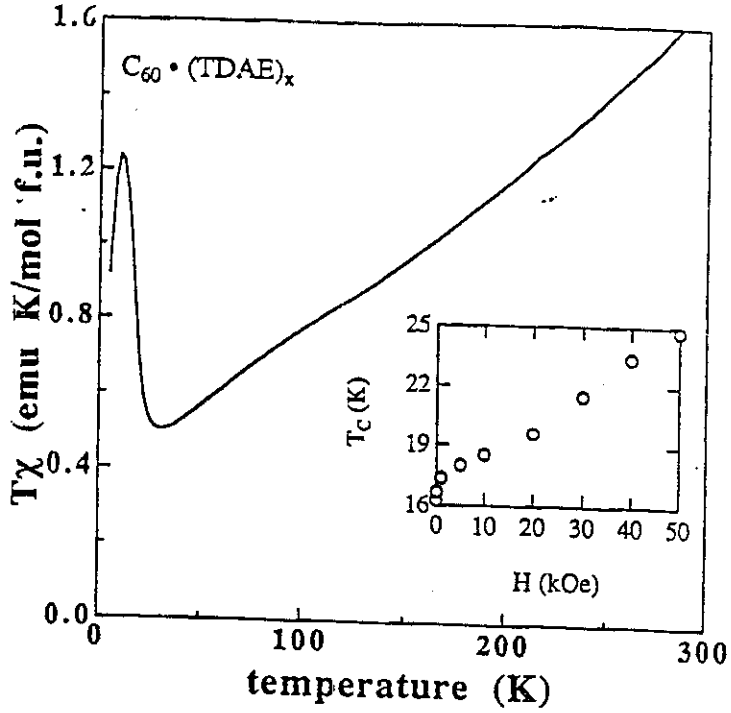

Microwave absorption in $K_x C_{60}$ S. Glarum

freq. ~ 9 GHz

surface impedance $\zeta = i\omega\lambda/c$

$1/\lambda^2 = (4\pi/c^2)(ne^2/m + i\omega\sigma) = i/\lambda_L^2 + 1/\delta^2$

London penetration depth

skin depth

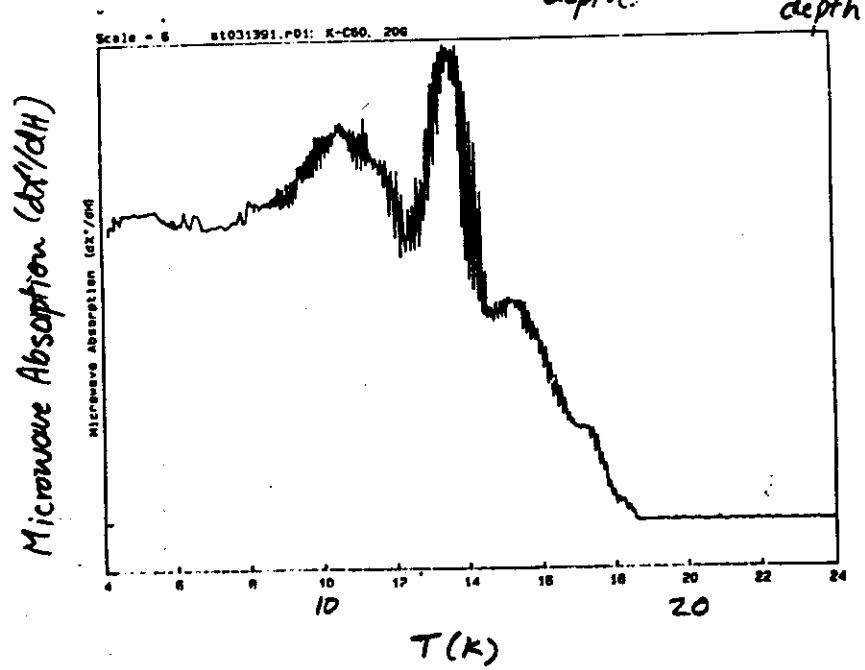

Stoichiometry and Diamagnetic Shielding

Holczer et al., Science 252, 1154 (1991)

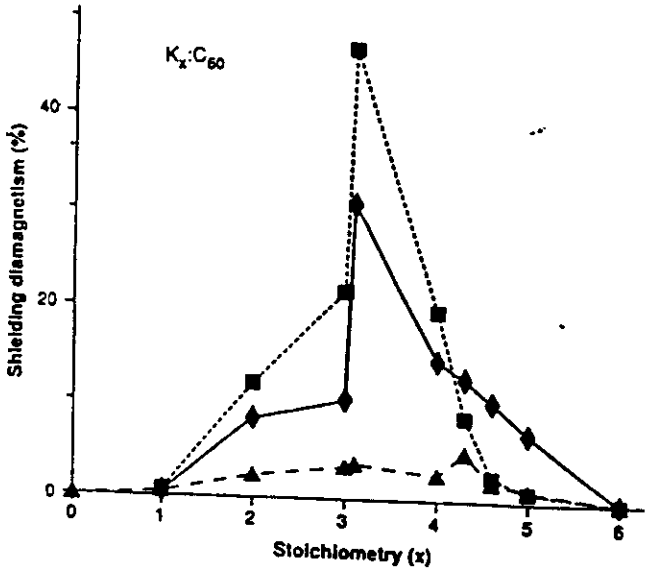

Use pressure-dependence to estimate Bulk Modulus (B)

Skjinber et al (Sandia)

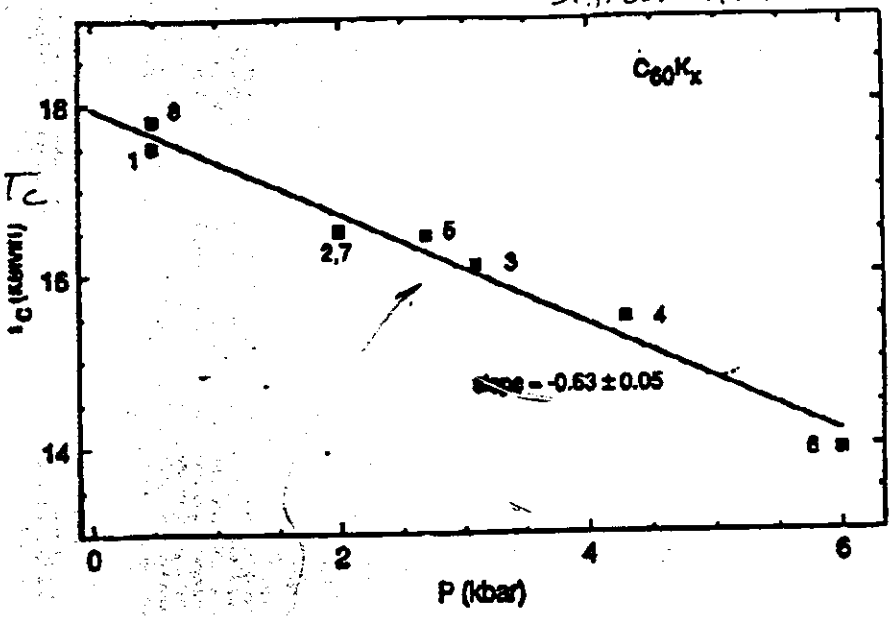

$$\frac{\partial T_c}{\partial P} = -0.63 \frac{K}{kbar}$$

$$\frac{\partial T_c}{\partial V} = 0.088 \frac{K}{\text{Å}^3} \quad \text{(from } K_{3-x}Rb_x \text{ doping)}$$

$B_{A_3C_{60}} \simeq 36$ GPa

$B_{C_{60}} \simeq 18$ GPa (Duclos)

$\therefore$ A_3C_{60} is twice as "stiff" as C_{60}.

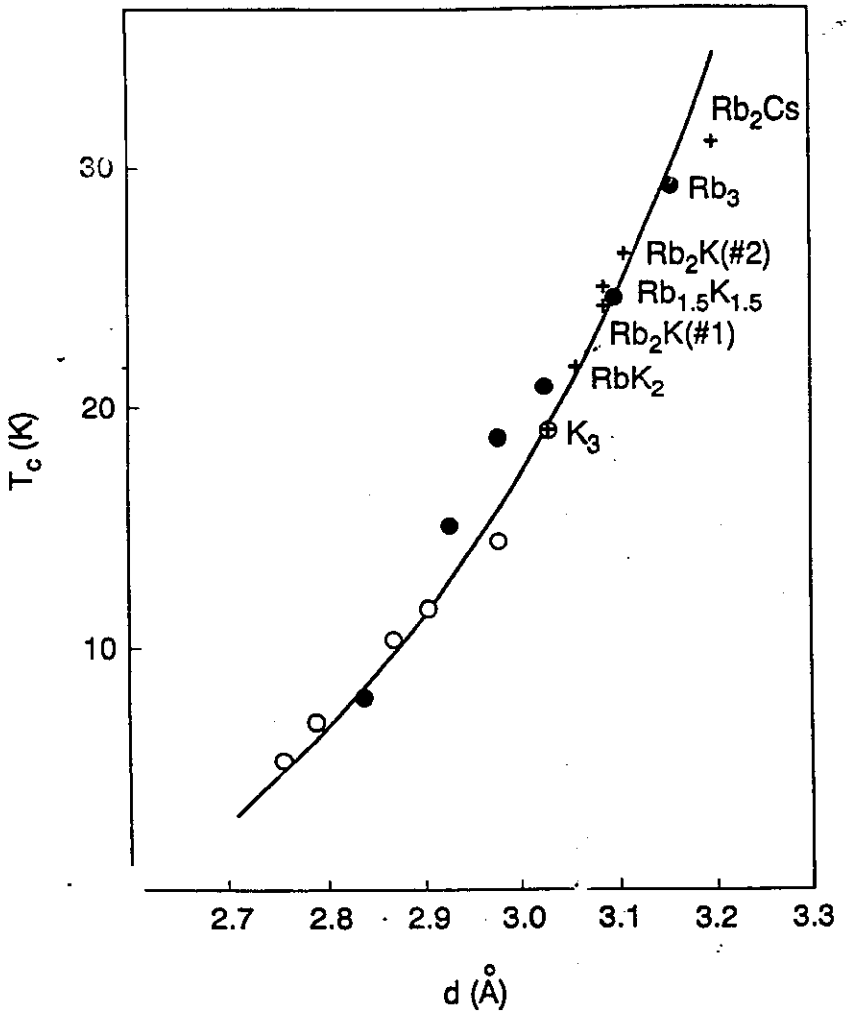
Rb_2Cs
Rb_3
$Rb_2K(\#2)$
$Rb_{1.5}K_{1.5}$
$Rb_2K(\#1)$
RbK_2
K_3
30
20
10
T_c (K)
2.7
2.8
2.9
3.0
3.1
3.2
3.3
d (Å)

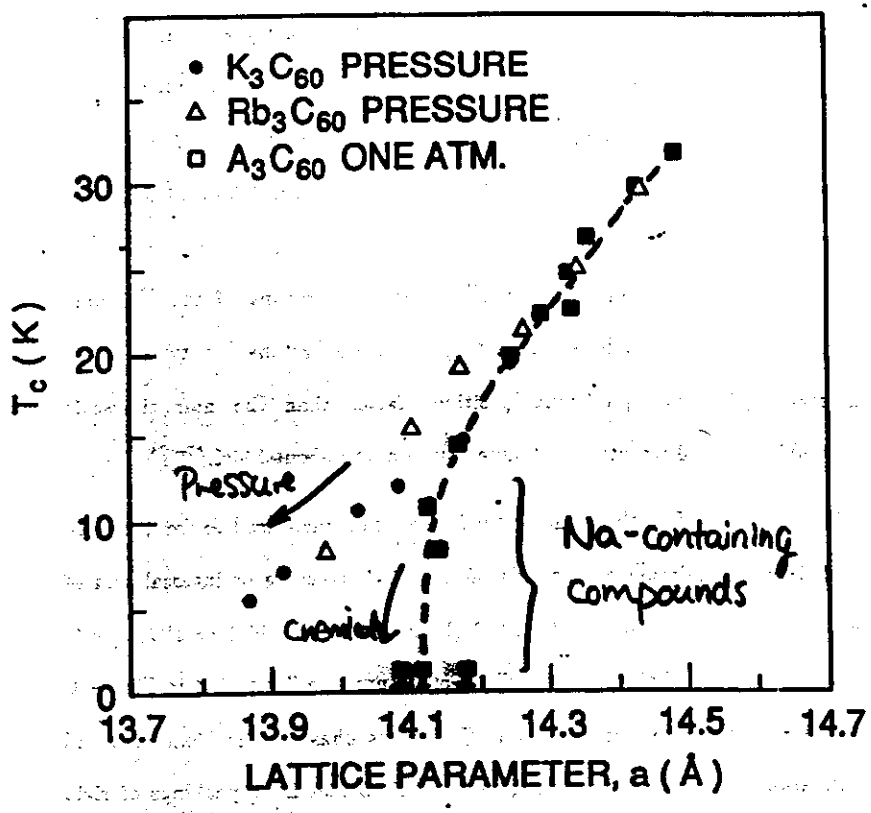
K_3C_{60} PRESSURE
Rb_3C_{60} PRESSURE
A_3C_{60} ONE ATM.
30
20
10
0
T_c (K)
Pressure
Chemical
Na-containing compounds
13.7
13.9
14.1
14.3
14.5
14.7
LATTICE PARAMETER, a (Å)

FIGURE 7

What Controls T_c ?

Naive approach –

Lattice constant

⇩

Density of States

⇩

T_c

(via the usual phonon theories
– but need high ω)

Intermolecular Phonon-Mediated Pairing

Zhang, Ogata + Rice, PRL 67, 3452 (1991)

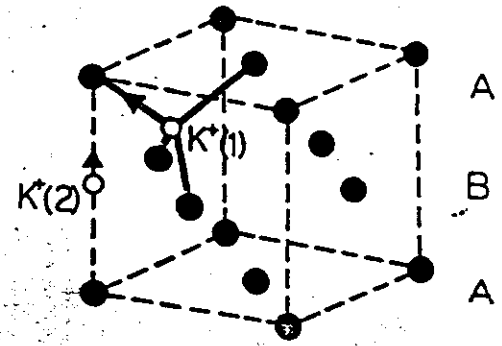

FIG. 1. The fcc lattice structure of K_3C_{60}. Solid circles represent C_{60}^{3-} molecules. They are surrounded by eight $K^+(1)$ at the center of the tetrahedron consisting of four nearest-neighbor C_{60} and six $K^+(2)$ located at the middle of every two next-nearest-neighbor C_{60}. Only one of each is shown by an open circle. The ratio of $K^+(1)$ and $K^+(2)$ sites is 2:1. The arrows indicate K^+ motion toward the more negatively charged C_{60}. *A* and *B* represent the two sublattices for CDW consideration.

- K^+-ion optic phonons strongly couple to electrons
- fcc lattice frustrated ∴ superconductivity is favored over a CDW state.

The $(K,Rb)_3C_{60}$ study begs the questions:

How far can the lattice be pulled apart ?

What are the neighboring structures ?

Are they superconducting ?

Forming a microscopic description of Superconductivity

McMillan equation

$$T_c = \frac{\langle\omega\rangle}{1.2} \exp \frac{-1.04(1+\lambda)}{\lambda - \mu^*(1+.62\lambda)}$$

$\langle\omega\rangle$ - frequency of "phonons"

λ - elect.-phon. coupling strength ($=N_0V$)

μ^* - elect-elect. interaction

Need to place bounds on $\langle\omega\rangle$, λ, μ^*.

Current Theoretical Models for pairing in A_3C_{60}

- Intramolecular phonons

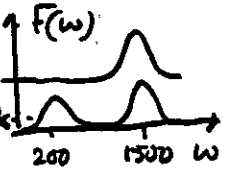

  - Varma, Zaanen + Raghavachari
  - Schluter, Lannoo, Needels + Baraff + Tománek

↑ ↑ λ μ^* - $\omega \sim 1400$ K (H_g) modes (intraball)

$N \sim 10$ states/eV spin C_{60} (interball)

- Intermolecular phonons

↑ ↑ λ μ^*
  - Zhang, Ogata + Rice
  - Negative U from K-optic phonon ($\omega \sim 200$ K)
  - SC stabilized vis a vis CDW by frustration

- Electron-Electron pairing

↑ ↑ λ μ^*
  - Chakravarty + Kivelson
  - Negative U results from spin-charge decoupling in an RVB state.
  - Baskaran + Tosatti

λ μ^* electronic depends on μ^*

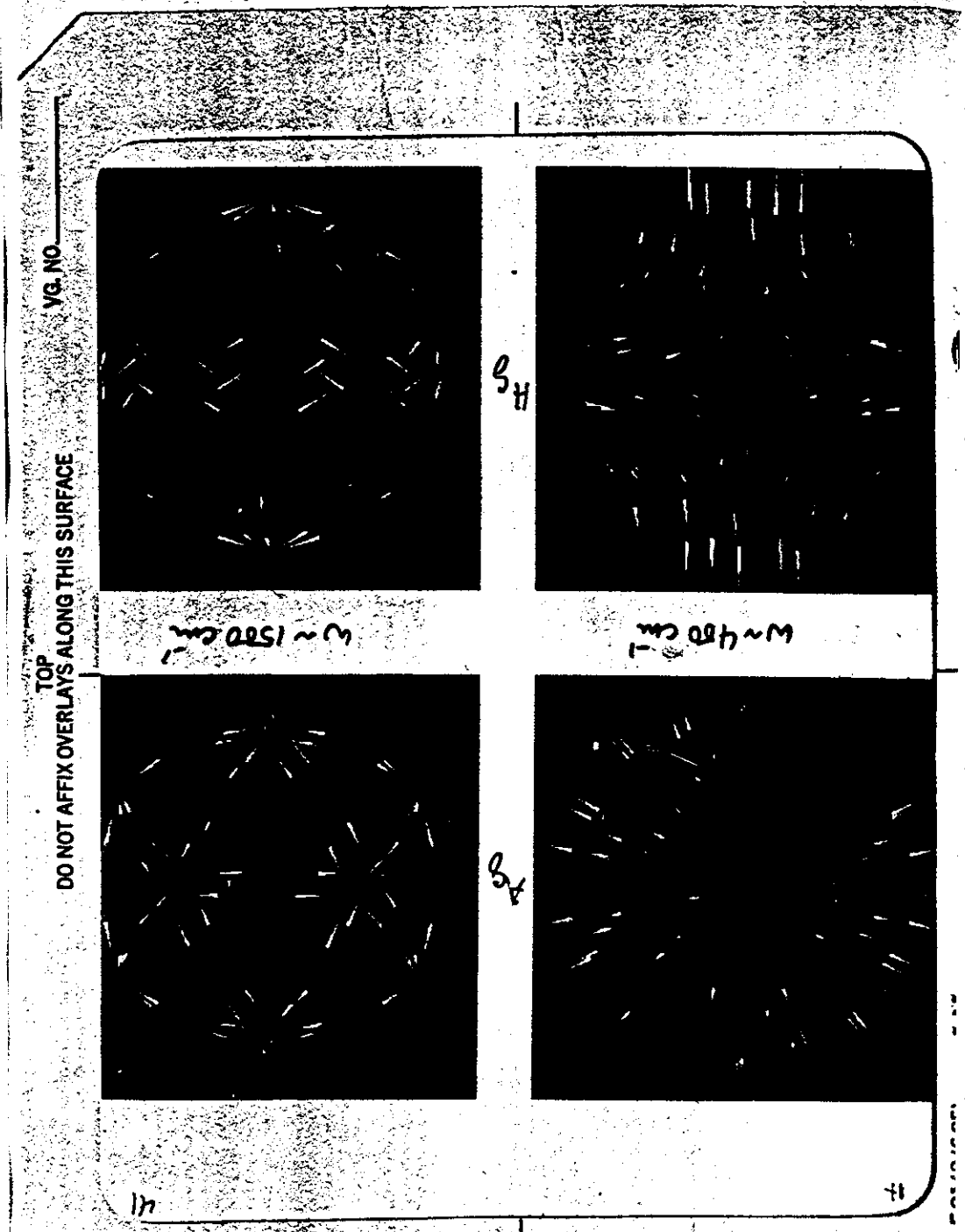

Electronic Correlations, Superconductivity in A_xC_{60}

Chakravarty, Kivelson, Gelfand, Science 254, 970 (1992)

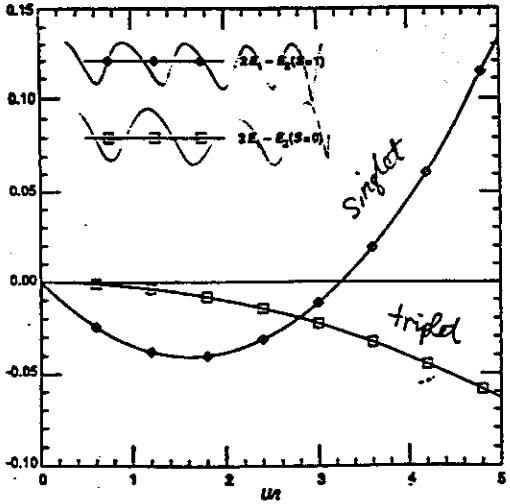

Fig. 1. The C_{60} singlet and triplet E_{pair} (in units of t) as functions of U/t for $t' = t$.

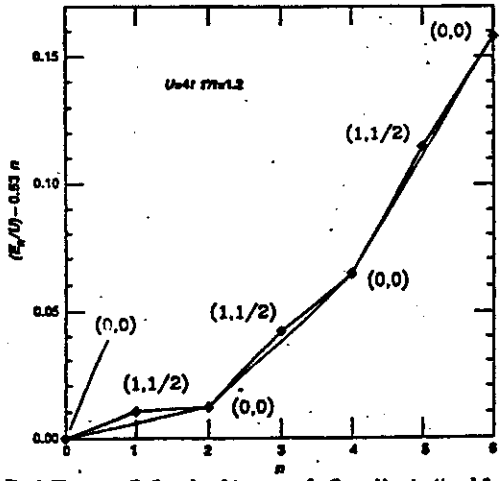

Fig. 2. The energy E_n (in units of t) versus n, for C_{60} at $U = 4t$, $t'/t = 1.2$. Note that a linear piece has been subtracted for clarity. The values of L and S for the lowest energy states at each n are indicated in the form of (L, S).

Our Approach

- Assume for the present the interaction is mediated by phonons (evidence to follow)
- Measure and analyze thermo-magnetic data χ, ΔC in terms of phonons (HcM eqn.)
- Does this approach fail?
- Hope to distinguish between high- and low-energy phonons (inter, or intra).

Inelastic Neutron Scattering

Prassides et al, Nature 354 462(1992)

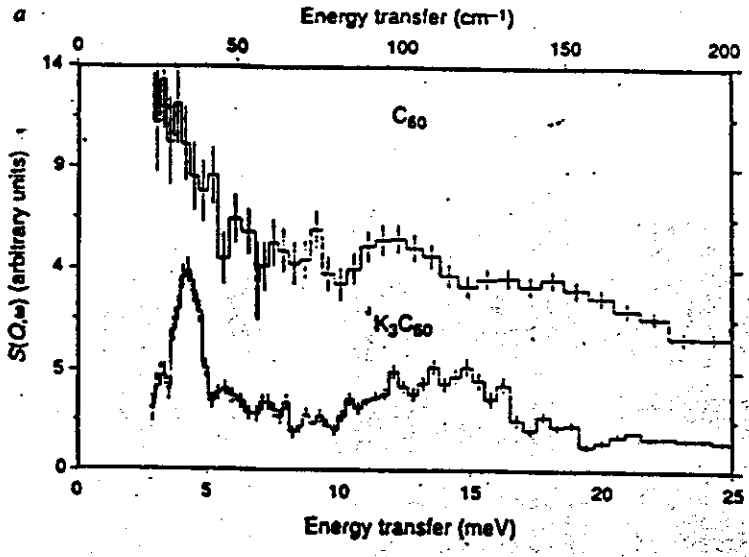

FIG. 1 Inelastic neutron scattering spectra in the energy regions (a) 0–25 meV and (b) 25–200 meV of C_{60} at 20 K (top) and K_3C_{60} (bottom); the K_3C_{60} data were collected at 5 K and 30 K and summed. The instrumental

- Significant changes in peak positions + intensities on doping.
- Buckling modes $H_g^{(2)}$, $H_g^{(8)}$ disappear

Effect of Alkali doping on Vibrational modes

Duclos et al

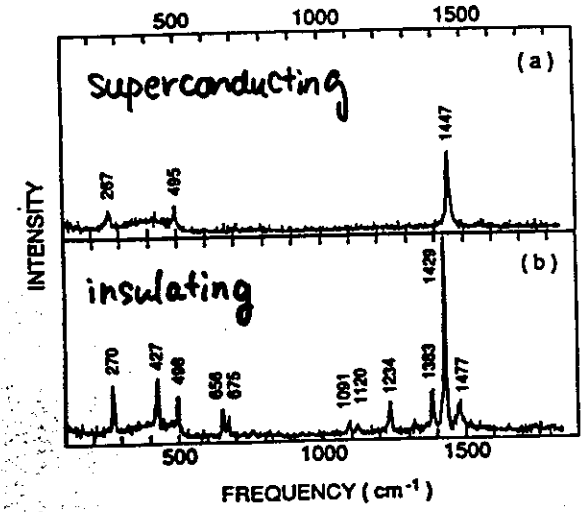

Figure 4. In situ Raman spectra of a C_{60} film taken during rubidium doping: (a) superconducting and (b) insulating.

Tatu

C_{60} fulleride Raman spectroscopy

Room temperature

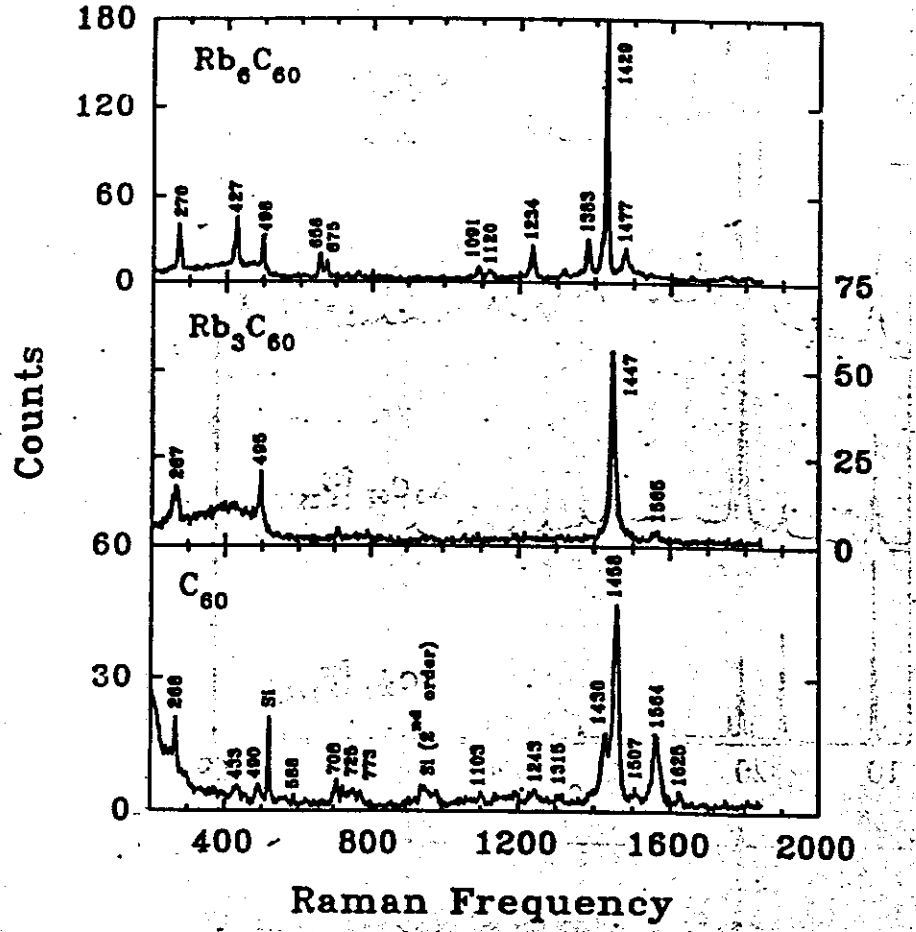

Isotope Effect (APR et al PRL, Feb 92)

- Can distinguish between phononic ($T_c \propto M^{-\alpha}$) and electronic mechanism.
- Use α along with T_c to determine λ, μ^*, for a given $\langle\Omega\rangle$.

Intermediate Coupling $\lambda < 1$ (McMillan)

$$T_c = \frac{\langle\Omega\rangle}{1.2}\exp\left[-\frac{1.04(1+\lambda)}{\lambda-\mu^*(1+0.62\lambda)}\right]$$

$$\alpha = -\frac{\partial \ln T_c}{\partial \ln M} = \frac{1}{2}\left[1-\left\{\mu^* \ln\frac{\langle\Omega\rangle}{1.20T_c}\right\}^2 \frac{1+0.62\lambda}{1+\lambda}\right]$$

Strong Coupling $\lambda >> 1$ (Kresin)

$$T_c = 0.18\lambda^{\frac{1}{2}}\langle\Omega\rangle.$$

$$\alpha = \frac{1}{2}\left[1-\frac{1.3\mu^{*2}}{1+2.6\mu^*}\right]$$

Isotope Effect Sample Preparation

- Mix 75% (weight) ^{13}C powder with 25% ^{13}C (universally labelled) Glucose.
- Press @ 14kbar, a 1/4" rod.
- Heat to 250C to polymerize the glucose.
- Graphitize at T > 2500 C.
- Standard procedure for synthesising C_{60}.
- 10 grams of rod yielded 37 mg C_{60}.
- Prepared a control $A_3{}^{12}C_{60}$ sample, along with ^{13}C sample using Penn method.

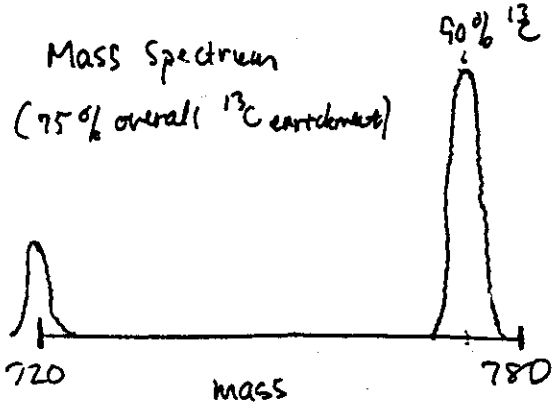

Raman Spectrum (Intramolecular modes)

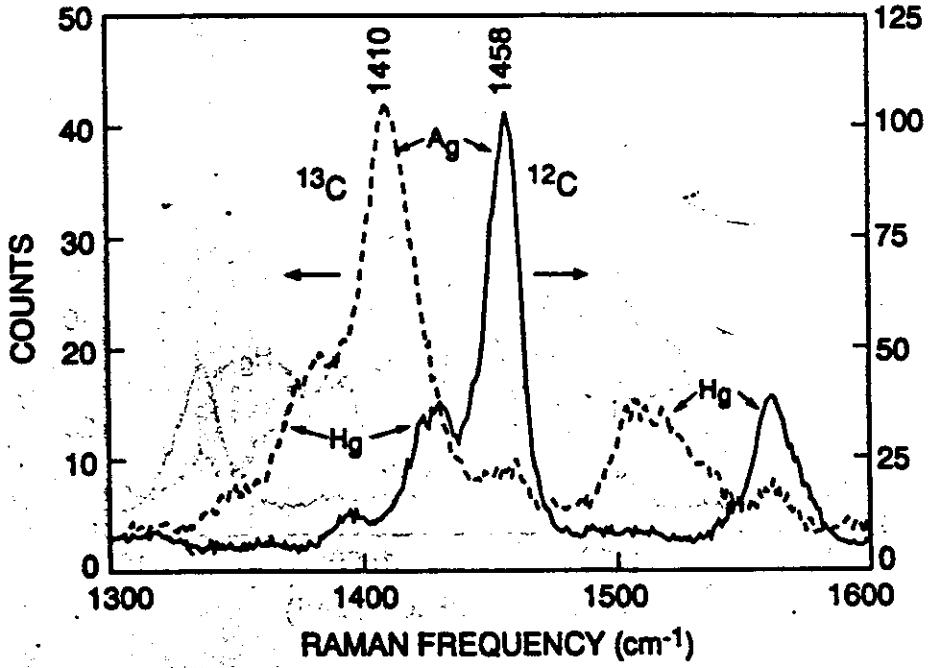

Isotope Shift in Rb_3C_{60}

Ramirez, Kortan, Rosseinsky, Duclos, Mujsce
Haddon, Murphy, Makhija, Zahurak, Lyons
PRL 68, 1058 (92)

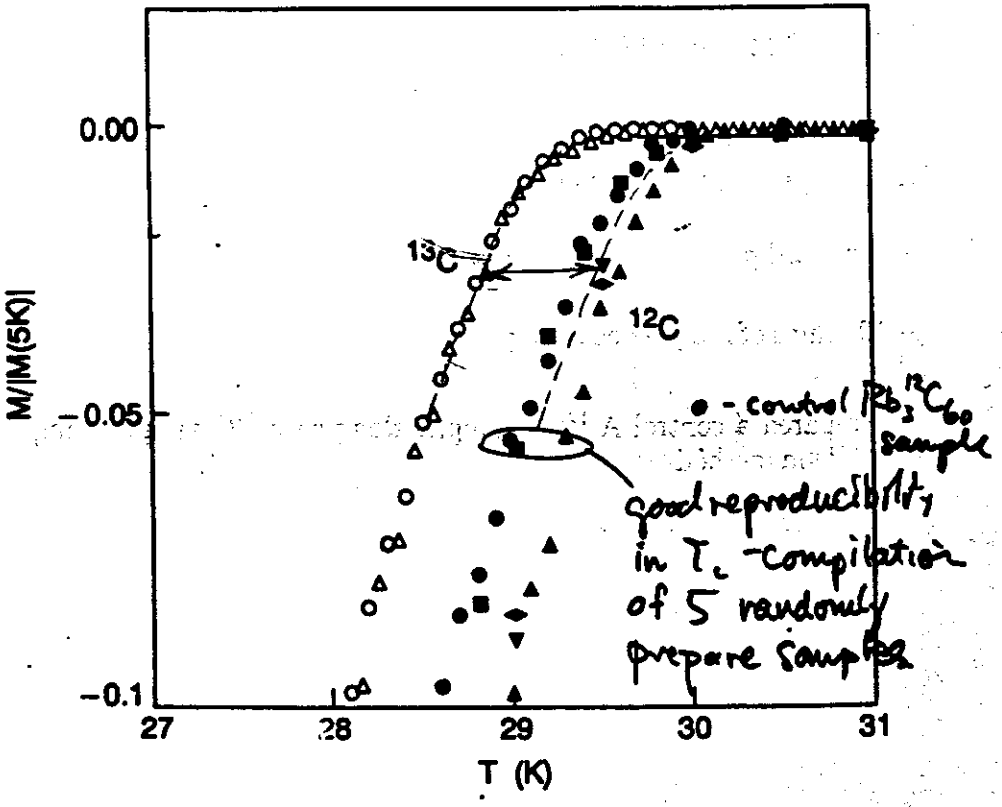

- High reproducibility of T_c good evidence for a line phase.

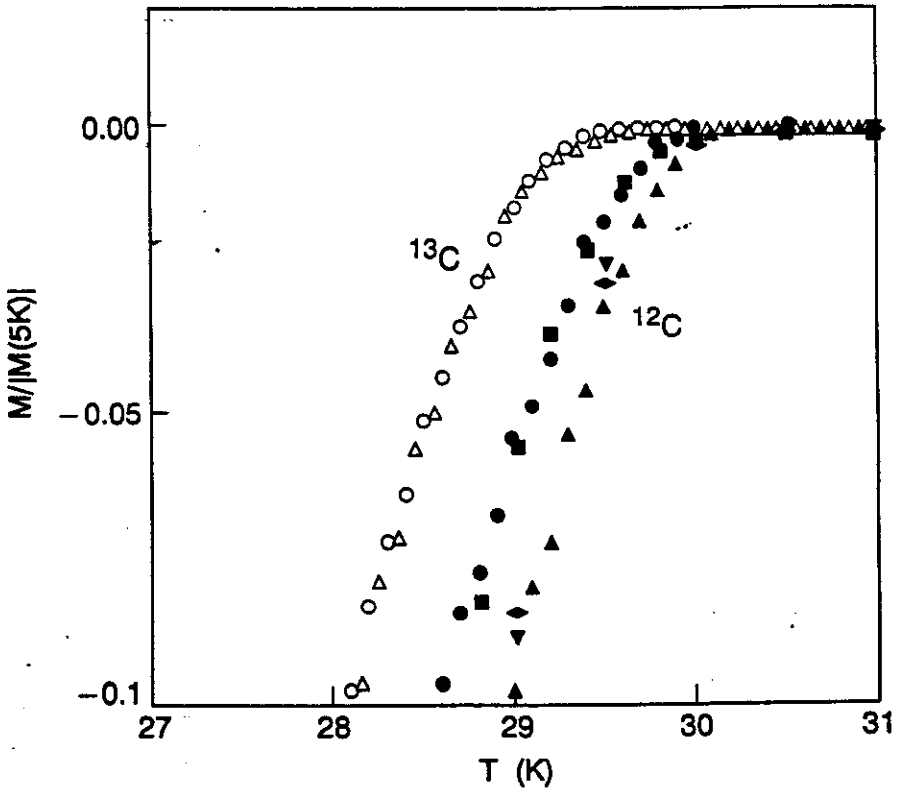

Fig. 2

Isotope Effect in $K_3{}^{13}C_{60}$

Chen + Lieber, J. Am. Chem. Soc., 114, 3141 (1992)

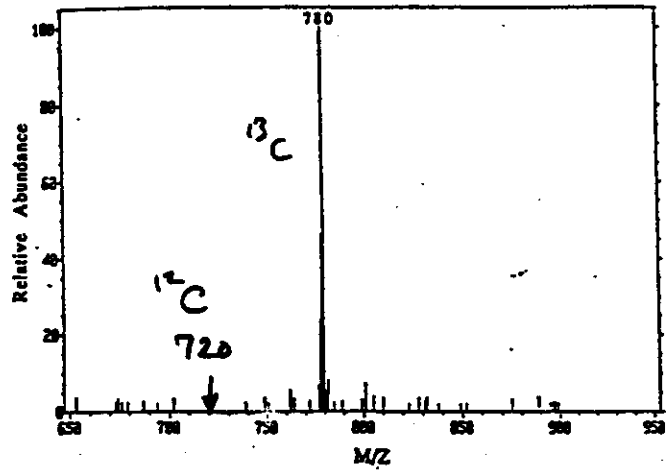

Figure 1. Field desorption (FD) mass spectrum of a purified $^{13}C_{60}$ sample (M^+, 780) recorded using a JEOL AX505H spectrometer. Experimental conditions were as follows: 30 mA FD emitter current; 3 keV ion energy; 9 keV extraction energy. Similar spectra were recorded using fast atom bombardment.

- 99% ^{13}C enrichment
- $\alpha \simeq 0.3 \pm 0.06$

Isotope Effect - Pb_3C_{60}

Ebbesen et al. Nature 355, 620 (1992)

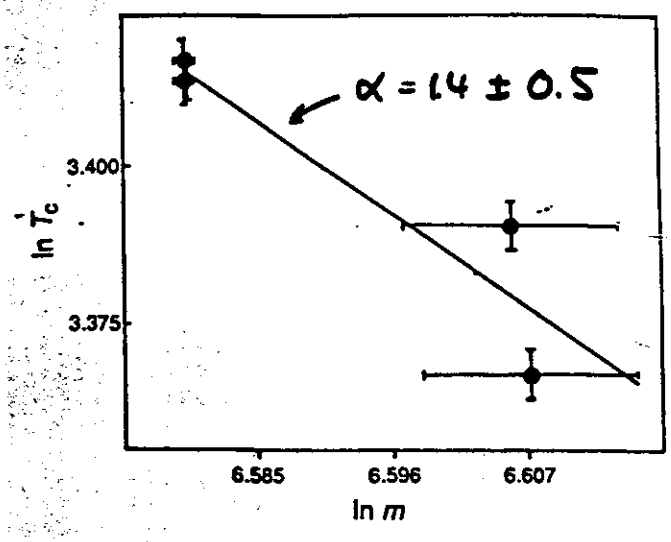

FIG. 3 Relationship between $\ln T_c$ and $\ln m$ (average C_{60} mass). The large horizontal error bars are due to the statistical spread of the C_{60} masses at a given average ^{13}C content.

- Samples only 33% enriched.

High-accuracy lattice constant determination

Fleming

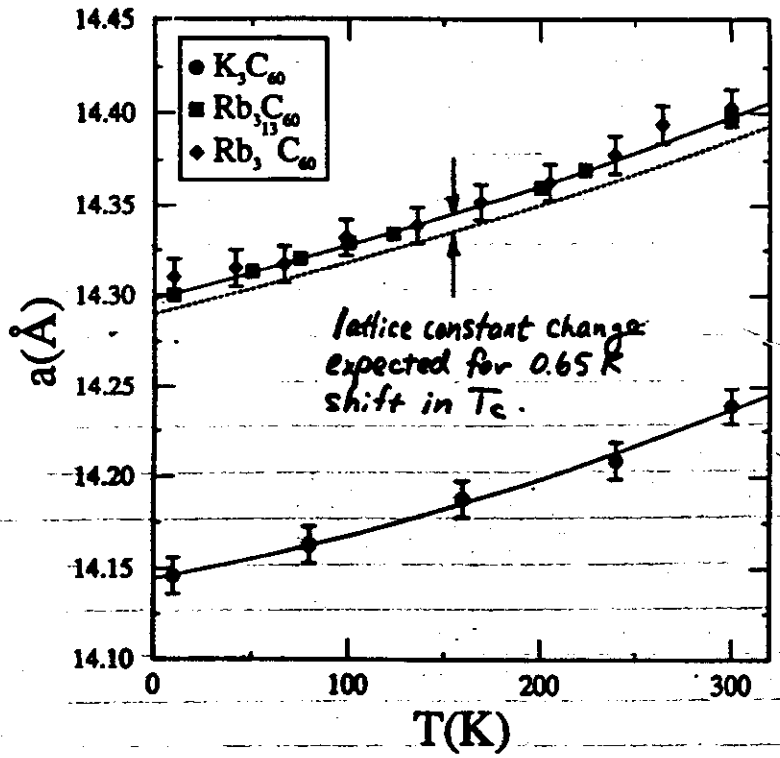

- Null result consistent with T_c shift driven by phonon-frequency change, not change in N_0 by zero-point fluctuation lattice change.

Isotope Effect — Conclusion

- After accounting for mass spectrum (75% overall enrichment) find

$$\alpha = 0.37 \pm 0.05$$

- If $\langle\Omega\rangle = 1400$ K, then find $\lambda = 0.72, \mu^* = 0.15$.
- If $\langle\Omega\rangle = 200$ K, then use strong coupling expressions, and find

$$\lambda > 2, \mu^* \approx 1.$$ (consistent w/ tunnelling)

- If $\langle\Omega\rangle = 200$ K from alkali optic modes, then

$$\alpha = 0.5(M_{Rb}/M_{C60})^{\frac{1}{2}} \approx 0.05$$ (unlikely)

- Conclude – T_c affected by phonons similar to regular phonon-coupled superconductors.
- Still can't say if weak or strong coupling.

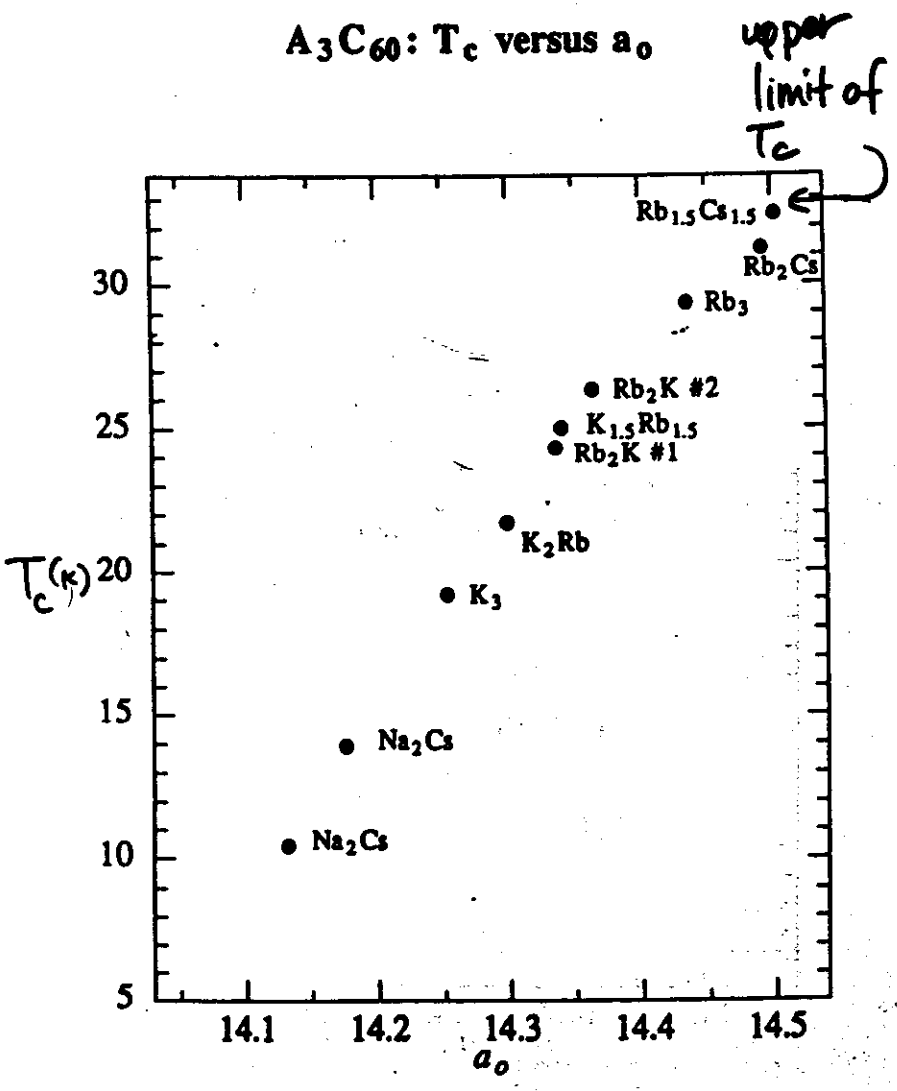

Chemical Tuning of T_c

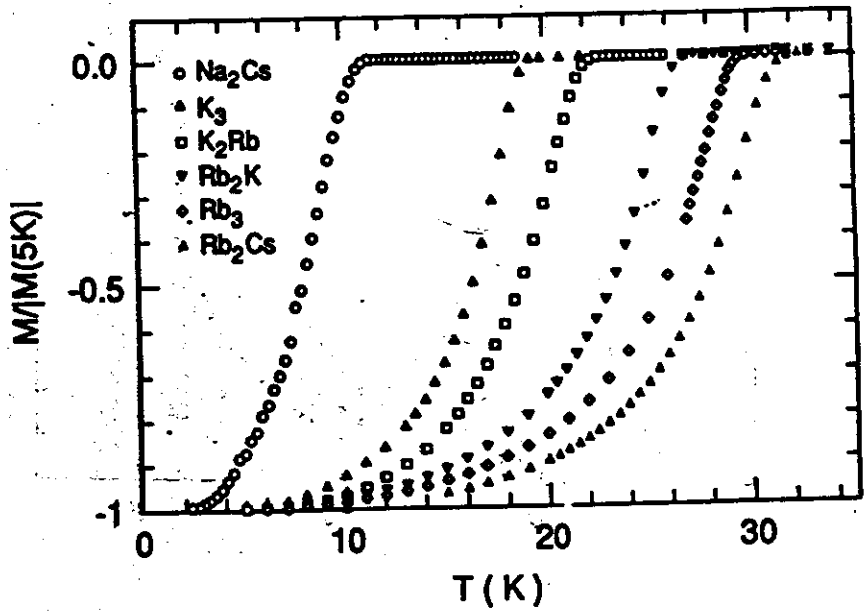

This suggests, via lattice-constant (a) change that the density of states (N) is driving T_c changes.

T_c vs. lattice parameter (FCC)

Fleming, Ramirez, Rosseinsky, Murphy, Haddon, Zahurak Mathija, Nature 352, 787 (1991)

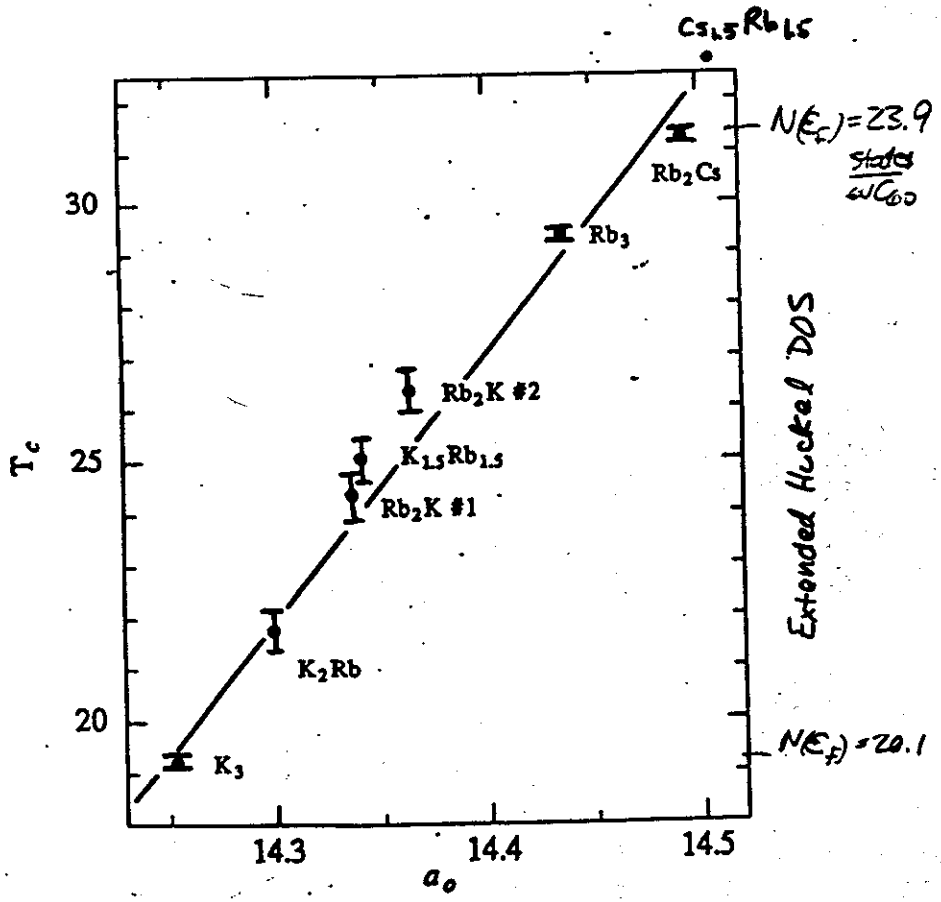

Density of States $N(E_F)$ from bulk $q=0$ measurements

Go back to free electrons

Pauli paramagnetic susceptibility χ_p

$$\chi_p = \mu_B^2 N^{\chi}(E_F)$$

Specific heat linear term $C = \gamma T$

$$\gamma = \frac{\pi^2}{3} k_B^2 N^{\gamma}(E_F)$$

Density of States N_o in A_3C_{60}

- Band structure → $W \approx 0.5$ eV → $N_o \approx 6$ states/spin-eV-C_{60}
- Extended Huckel theory → 20% increase, K to Rb.
- Parameters λ and μ^* not known well enough to predict T_c.
  However, can look at systematic trends, T_c vs. N_o.
- First, different measurements must be in agreement:
  XPS, NMR, X_p, C.

$$\chi_{pauli} = 2\mu_B^2 N_b (1-I)^{-1}$$

$$\gamma = \frac{2}{3}\pi^2 k_B N_b (1+\lambda+f(I))$$

- γ: specific heat $C = \gamma T$
- N_b: bare density of states
- $(1+\lambda+f(I))$: spin fluctuation mass enhancement
- λ: electron-phonon coupling strength

Density of States

$N(E_f)$

Chen et al

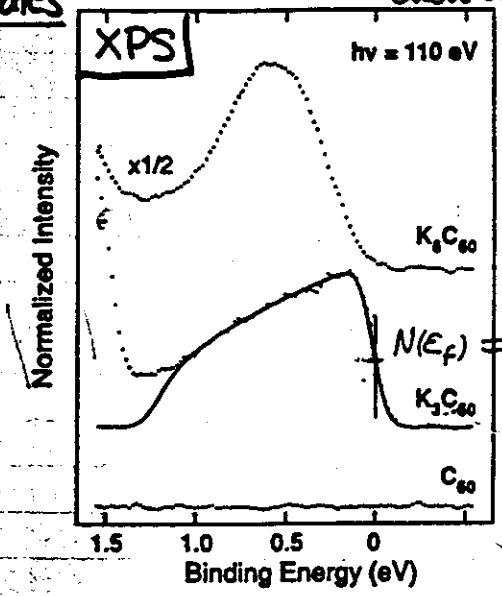

$N(E_f) = 1.9$ states/eV C_{60}

Science 253, 884 (1991)

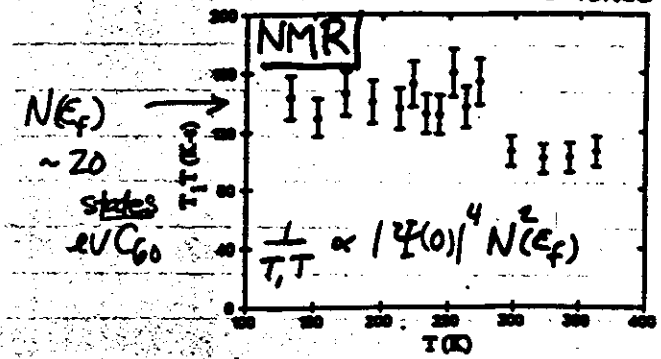

Fig. 4. Temperature dependence of the ^{13}C spin-lattice relaxation time T_1 in K_3C_{60}, plotted as T_1T versus T.

Upper Critical field in K_3C_{60}

Boebinger, Palstra et al., preprint

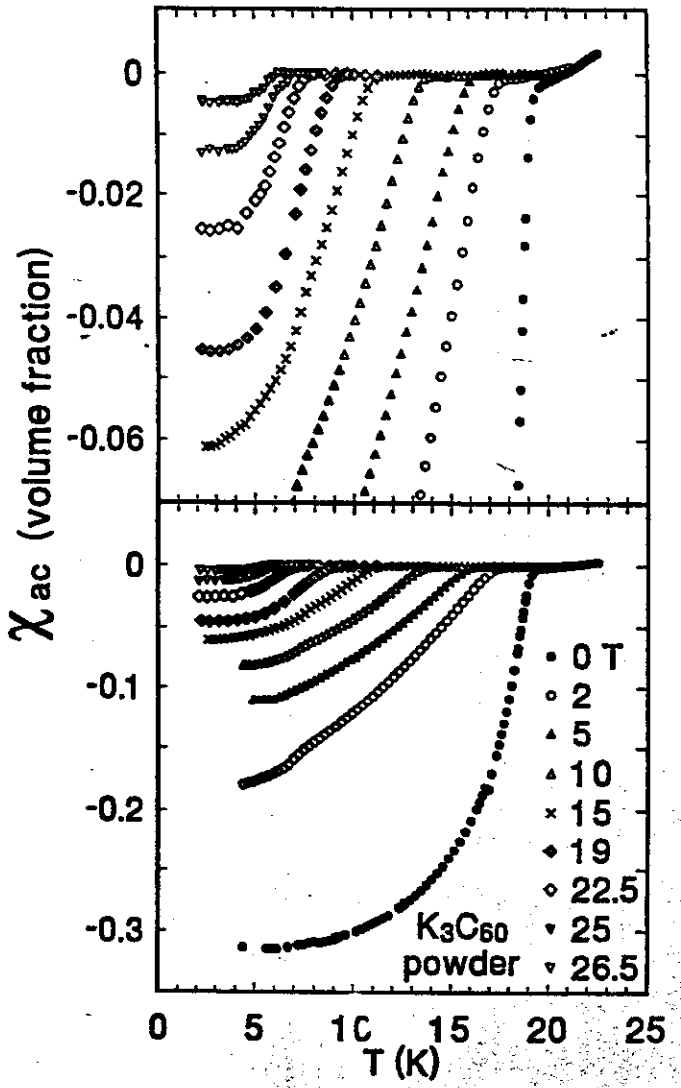

Upper Critical Field in K_3C_{60}

Boebinger, Palstra et al., preprint

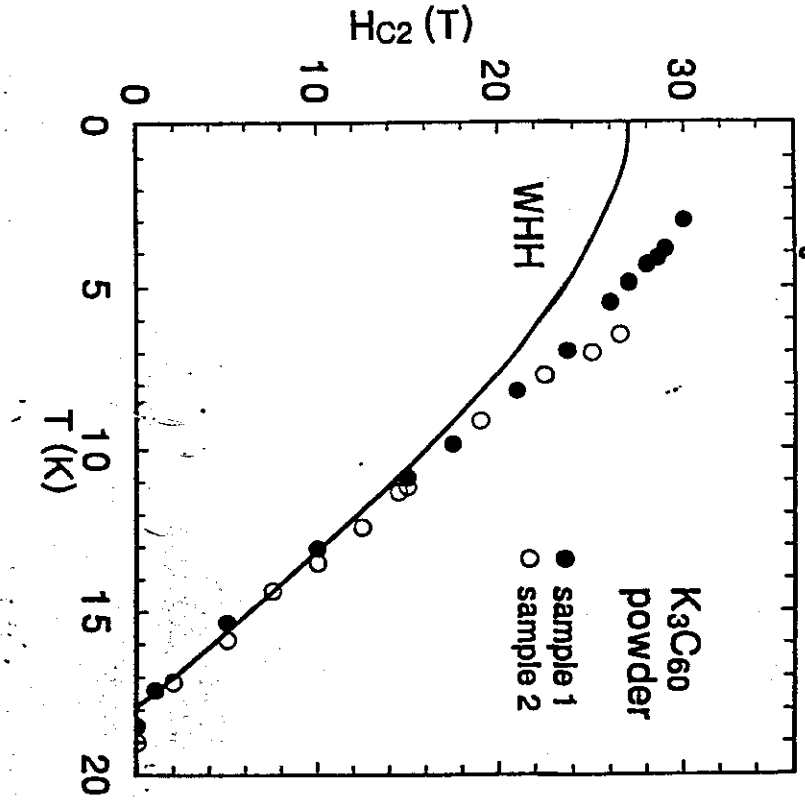

$(K Rb)_3 C_{60}$

This study begs question: how far can the lattice be pulled apart?
$Rb_2Cs C_{60}$ → $T_c \sim 33K$.

Also: what are neighboring structures? are they S.C.

Upper Critical Field in K_3C_{60}

Buckinger, Polstra, et al. preprint

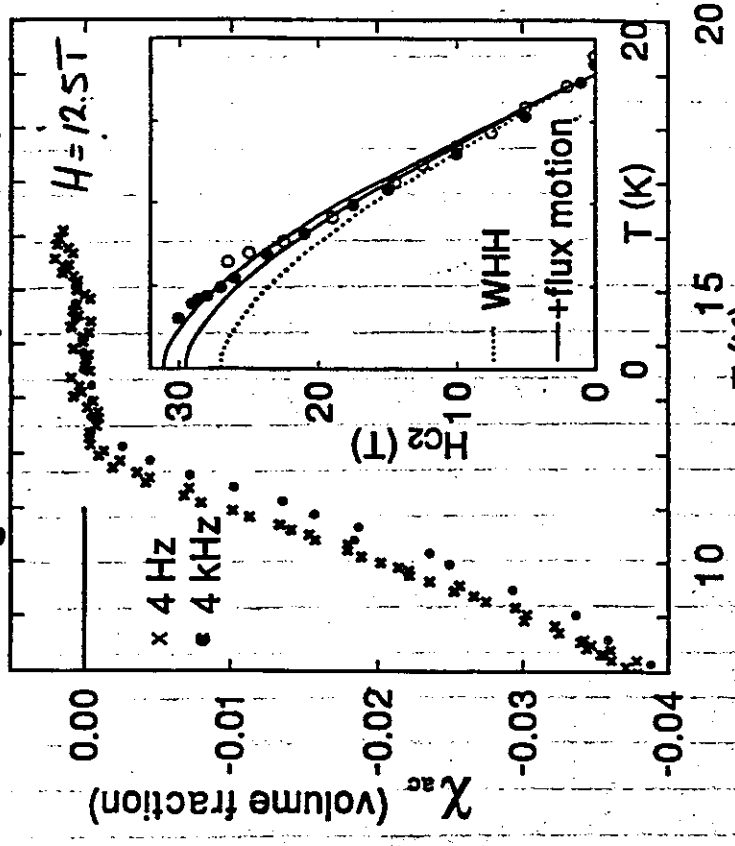

FIGURE (A)

Ring Currents in Icosohedral C_{60}

Pasquarello, Schlüter, Haddon, preprint

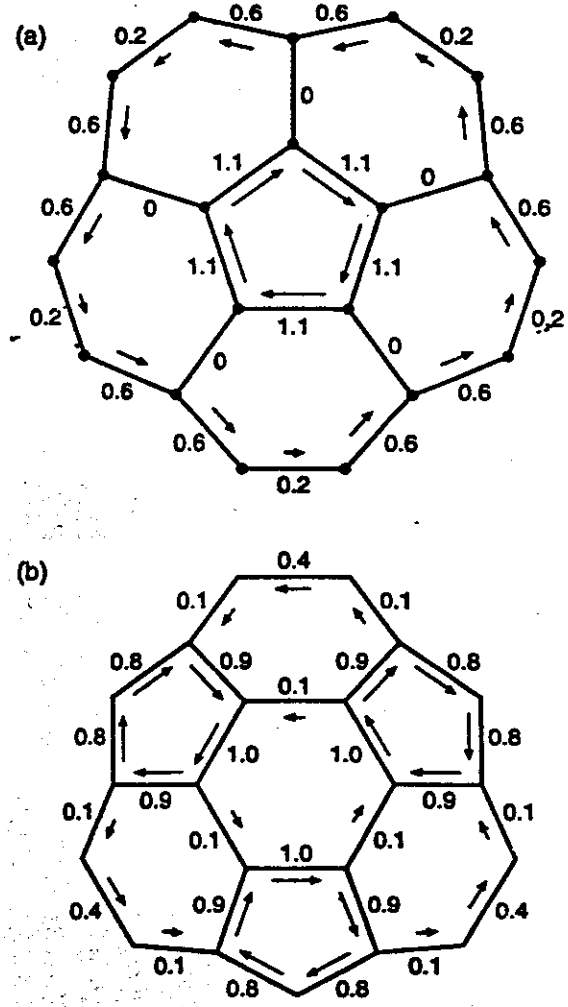

Figure 1

Ring Currents in Icosahedral C_{60}

Pasquarello, Schlüter, Haddon, preprint

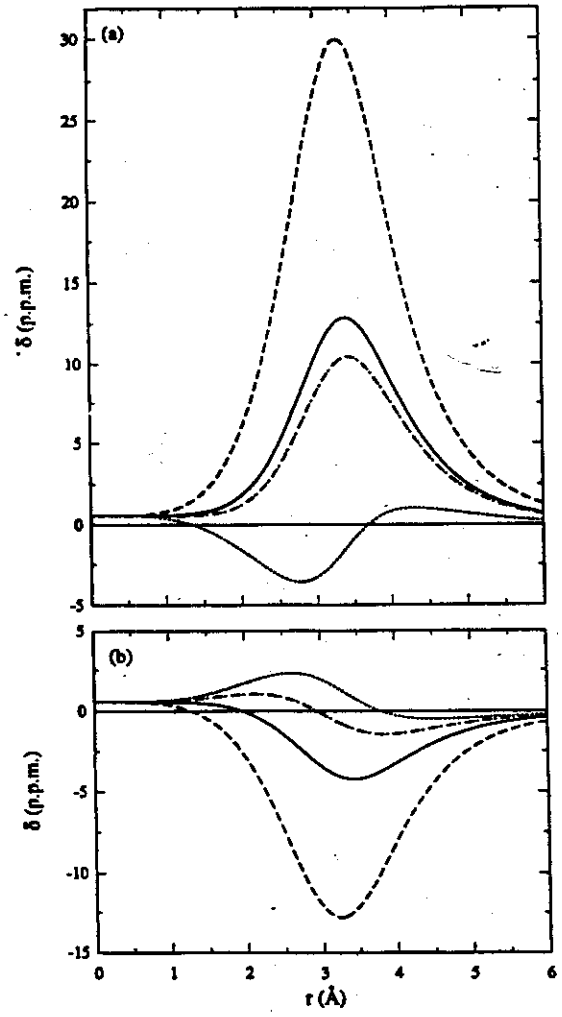

Figure 2

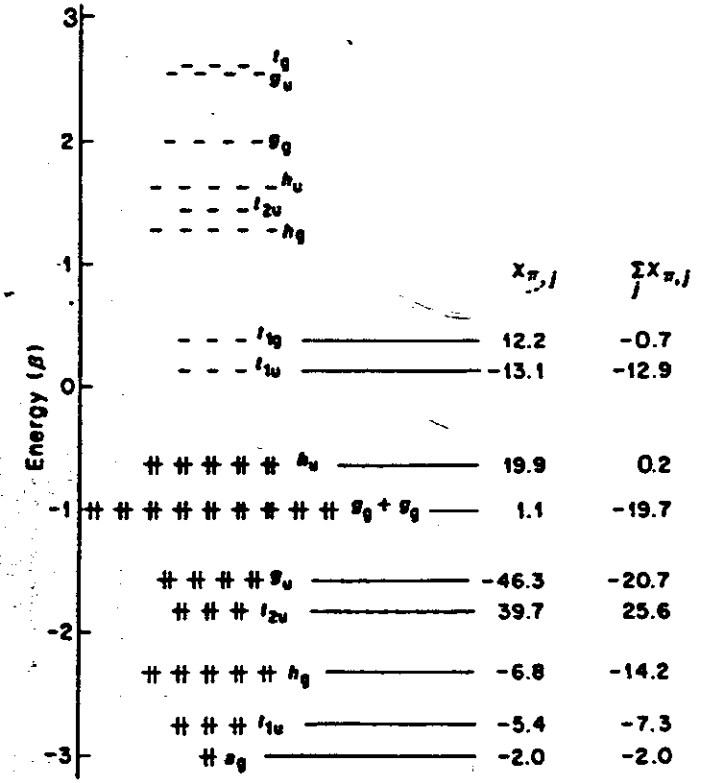

Fig. 2 Hückel molecular orbital[20], j, energy levels in units of β and π-orbital magnetic susceptibilities in units of $|\chi_\pi^{\text{benzene}}|$ calculated for C_{60} with a common resonance integral. Occupation of an orbital is denoted by a solid vertical line; labels refer to irreducible representations of the icosahedral point group.

Contributions to Normal State Susceptibility

$$\chi_{exp} = \chi_p + \chi_{orb} + \chi_L + \chi_{core}$$

- χ_p: Pauli spin susceptibility (+) — $\chi_p = \mu_B^2 N(E_F)$
- χ_{orb}: Conduction electron orbital (analogue of van Vleck) (+) — Orbital-energy denominator large — High symmetry (ring currents cancel (neglect))
- χ_L: Landau diamagnetism (−) — Landau - neglect for strong disorder (Is this reasonable?)
- χ_{core}: Core diamagnetism (−)

Core - atomic (alkali) + molecular (C_{60})

$\chi_{core} \simeq 80 + 260$ ppm $\cong \frac{1}{3}\chi_{exp}$

Normal State Susceptibility - K_3C_{60}, Rb_3C_{60}

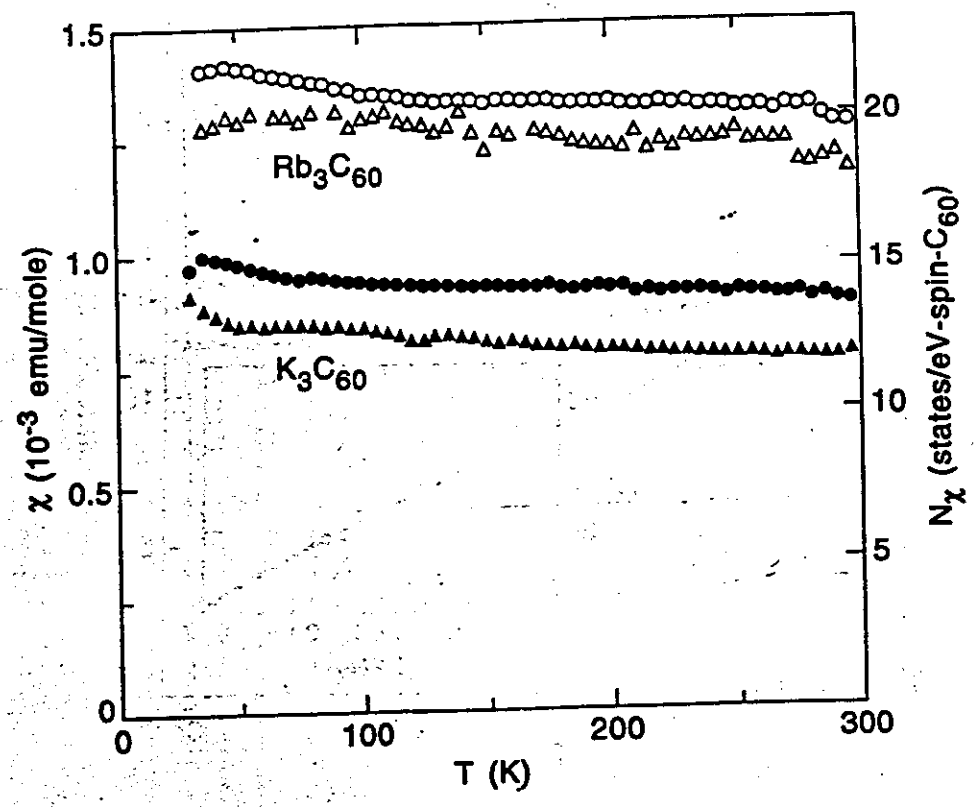

- Note large ~35-40% change in χ
- Compare to 14% change (Hückel)
  22% " (LDA)

Fig 1.

Density of States - T_c Relationship

Haddon, Accts. Chem. Res.

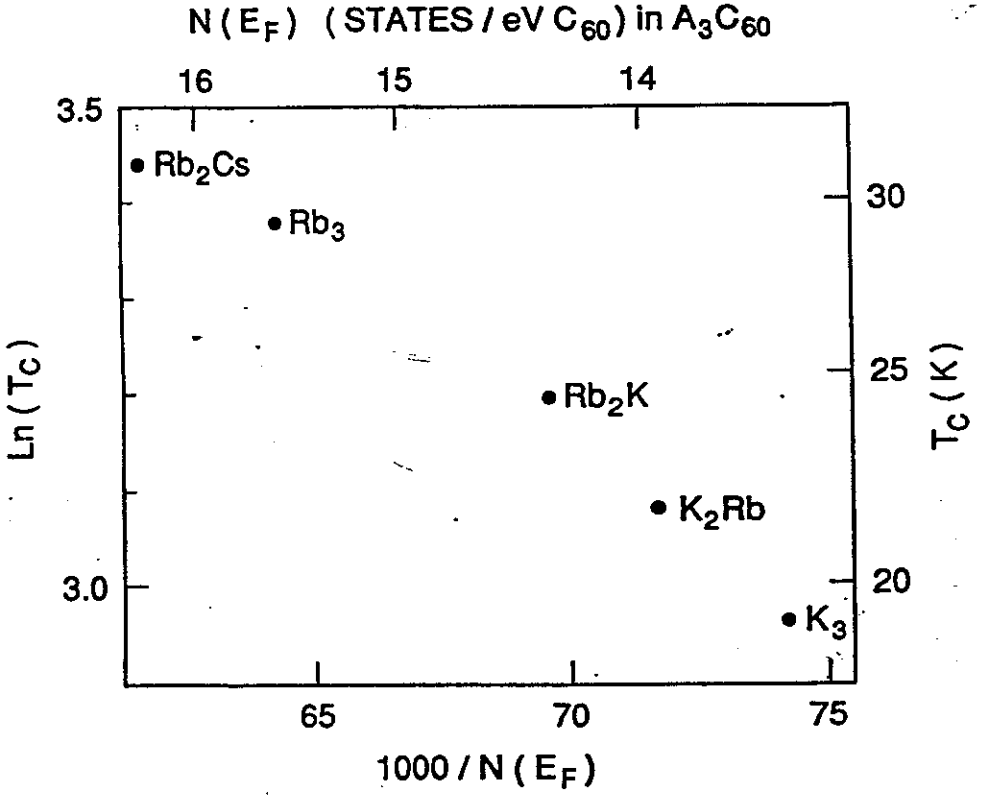

- DOS calculated by extended Hückel method
- $N_o(Rb_3C_{60})/N_o(K_3C_{60}) = \underline{1.14}$

Density of States – T_c Relationship

Oshiyama + Saito, Sol. St. Comm., 82, 41 (1992)

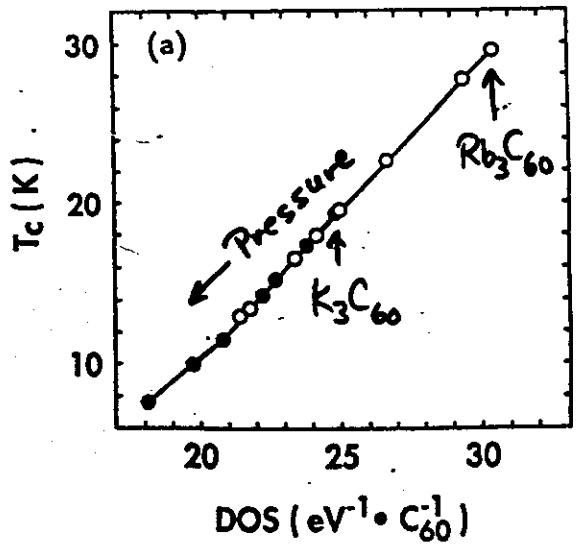

- DOS calculated w/ LDA using measured lattice constants
- $N_o(Rb_3C_{60})/N_o(K_3C_{60}) \approx 1.22$

Effect of Orientational Disorder on Electronic Structure

Gelfand - Lu, PRL, 68, 1050(1992)

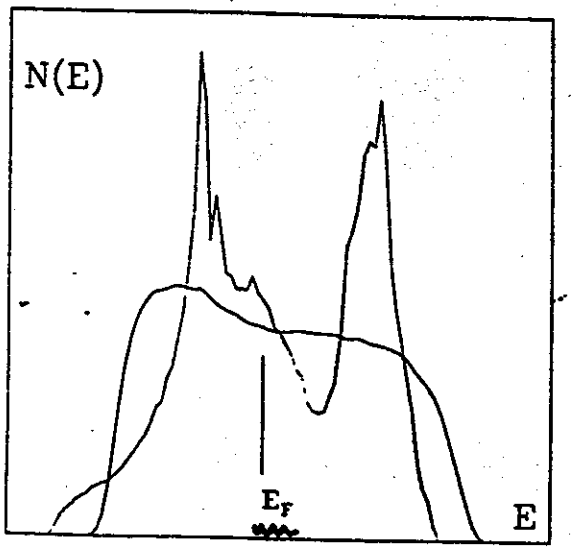

FIG. 3. Densities of states vs energy for the $Fm\bar{3}$ structure and its maximally disordered version; the former is the one with two large peaks. The Fermi energy for three electrons per molecule is indicated; it is nearly unchanged upon disordering.

- Use radial p_π (Hückel) orbitals
- Two inequivalent ($\pi/2$) orientations ⇒ vastly different hopping amplitudes (w.f. phase mismatch)
- Little effect on N_0

Variation of N within McMillan formalism

$$T_c = \frac{\langle\omega\rangle}{1.2} \exp\left[-\frac{1.04(1+\lambda)}{\lambda-\mu^*(1+0.62\lambda)}\right]$$

..... $\langle\omega\rangle = 1400$ K

—— $\langle\omega\rangle = 200$ K

---- $\langle\omega\rangle = 1400$ K and $N_\chi = \frac{N_0}{1-IN_0}$ $I \sim .05$

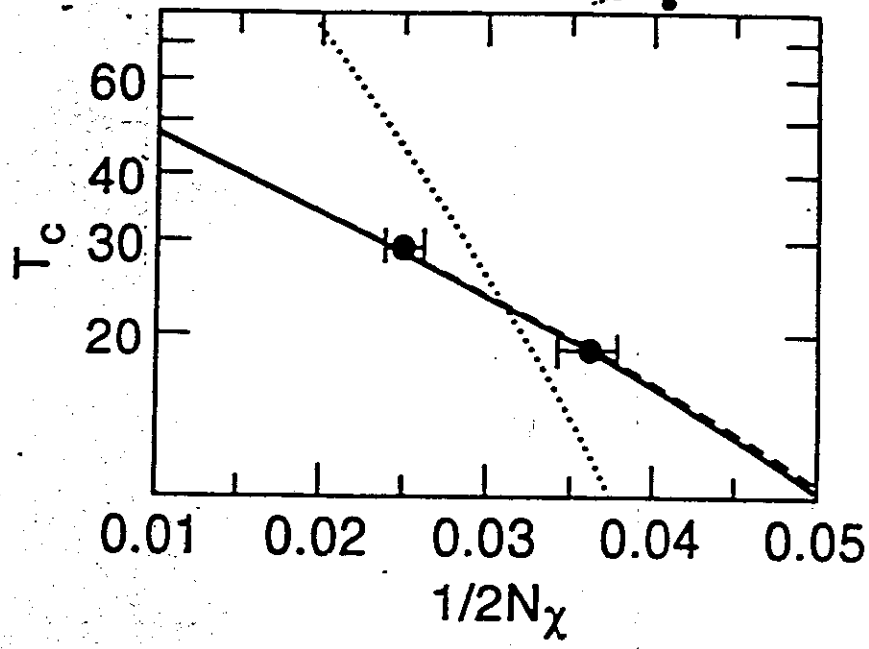

One way to explain large $N(E_F)$ changes

Stoner enhancement –

$$N_{meas} = \frac{N_{bare}}{1 - I N_{bare}}$$

N_{meas} = measured density of states

N_{bare} = bare density of states (N in McMegn.)

Then, assuming $T_{sf} = 1400$ K, get 2-3 enhancements of N.

N_{bare} (K) ≈ 4-5 states/eV spin C_{60}

N_{bare} (Rb) ≈ 5-6 " " " "

"Explains" discrepancy between NMR, photoemission

Introduces extra parameter, relating to spin fluctuations - (effect on superconductivity?)

Resistivity of single crystal used in Thermopower measurement

Inabe et al., preprint

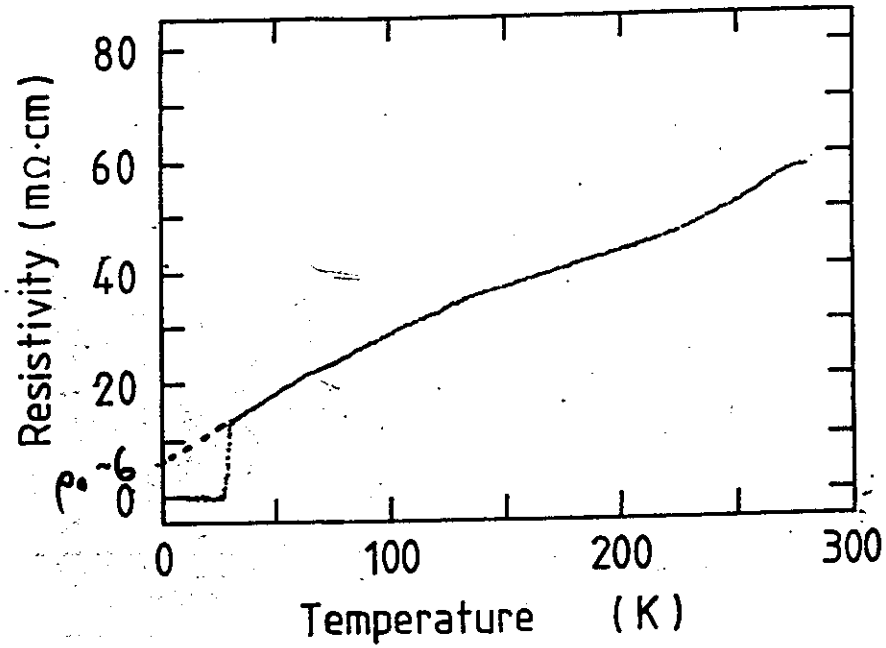

- Large $\rho_0 \sim 6 m\Omega$-cm illustrates problem of doping single crystals.

Thermopower in single crystal K_3C_{60}, Rb_3C_{60}

Inabe et al., preprint

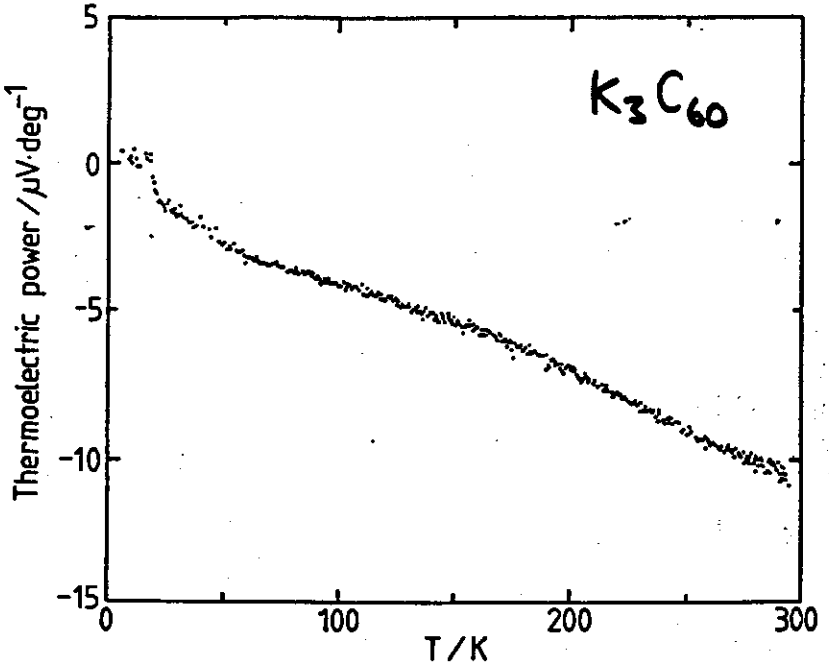

- $S(T) = \frac{\pi^2 k^2 T}{3e} \frac{1}{2E_f} \Rightarrow E_f \sim 0.35$ eV (electrons)

- $N_{RL} / N_k \sim 1.5 - 1.8$

Superconducting tunnelling (STM tip)
Zhang Chen, Kelty Dai + Lieber (Harvard)

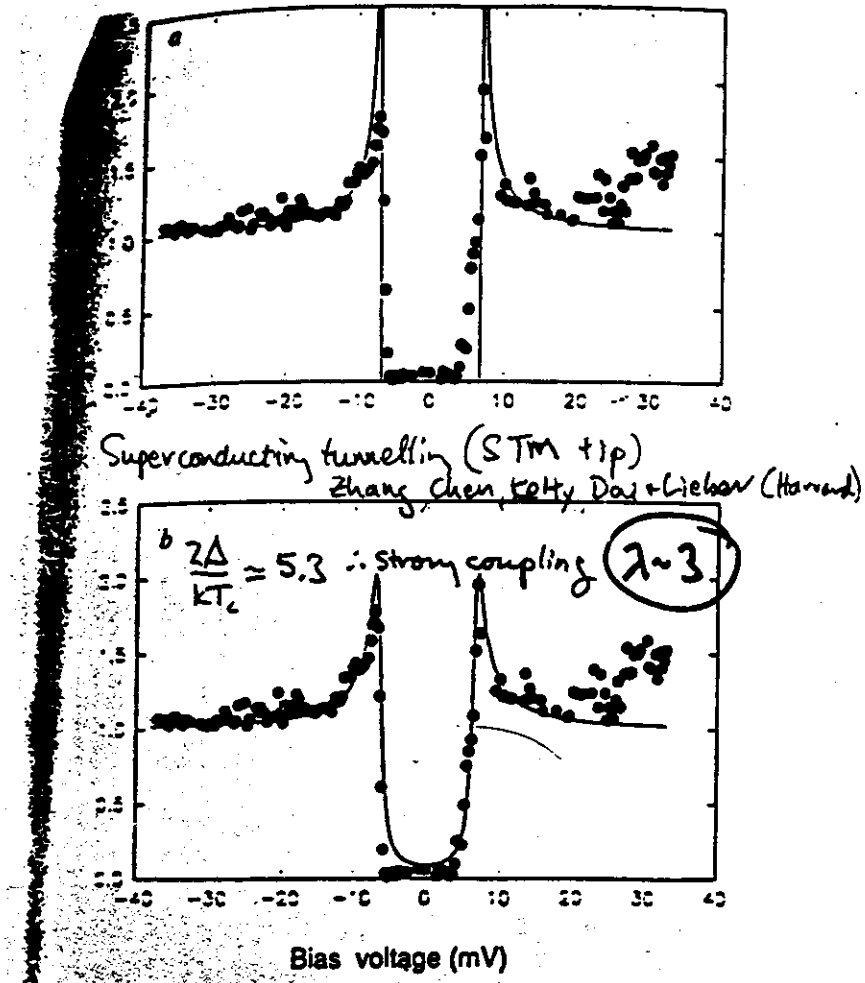

FIG. 3 Plots of dI/dV against voltage (mV) for Rb_3C_{60} at 4.2 K. The experimental data for conductance (solid circles) were calculated numerically from the I–V data in Fig. 2a. a, The data are fitted with the expression $dI/dV = eV/[(eV)^2 - \Delta^2]^{1/2}$ (solid curve) with $\Delta = 6.8$ meV. b, The data are fitted with the expression $dI/dV = \mathrm{Re}[|eV - i\Gamma|/((eV - i\Gamma)^2 - \Delta^2)^{1/2}]$ which includes broadening by Γ. The values of Δ and Γ are 6.6 and 0.6 meV, respectively.

NMR

Tycho

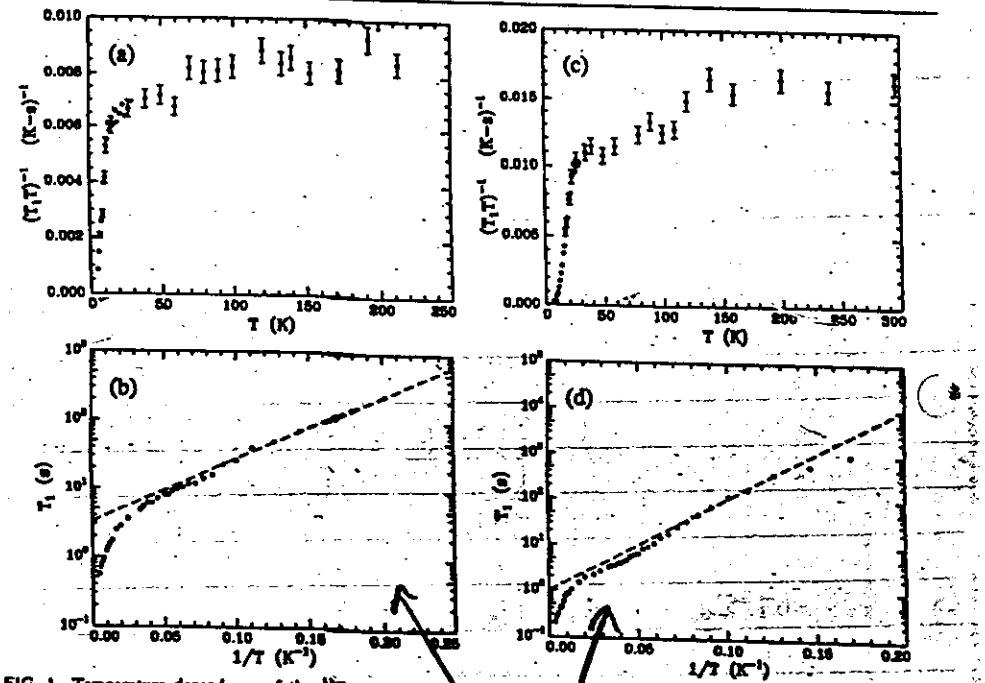

FIG. 1. Temperature dependence of the ^{13}C spin-lattice relaxation time T_1 in (a),(b) K_3C_{60} and (c),(d) Rb_3C_{60}, plotted as $(T_1T)^{-1}$ vs T [(a),(c)] and as $\log T_1$ vs T^{-1} [(b),(d)]. Error bars indicate 1 standard deviation. Dashed lines are fits of the data below 9 K [(b)] and from 8 to 12 K [(d)] by Arrhenius laws, leading to energy gaps $2\Delta^K \approx 42$ K and $2\Delta^{Rb} \approx 94$ K.

$\frac{2\Delta}{kT_c} \sim 3\text{-}4$

$\Downarrow$

$\lambda \sim 1$

Specific Heat Jump at T_c

- Can distinguish between strong and weak coupling.

  $\Delta C \propto 1.43(1+\lambda^2)$. (see graph)

- Critical field technique found $\Delta C = 90 \pm 15$ mJ/mole-K^2, consistent with BCS relation $\Delta C = 1.43\gamma$ and χ_P.

- Want to measure directly to check value.

- Use adiabatic technique. (good accuracy)

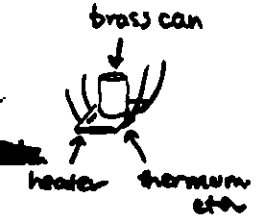

- [redacted]

Sample quality (K_3C_{60})

- Neutron Rietveld refinement - < few % 2nd phase
- NMR - < few % 2nd phase (no detectable C_{60}^{-} signal)
- Diamagnetic shielding ~ 35 % among the highest measured for a powder sample, and consistent with 100% transformed fraction. Measured before + after - no change.

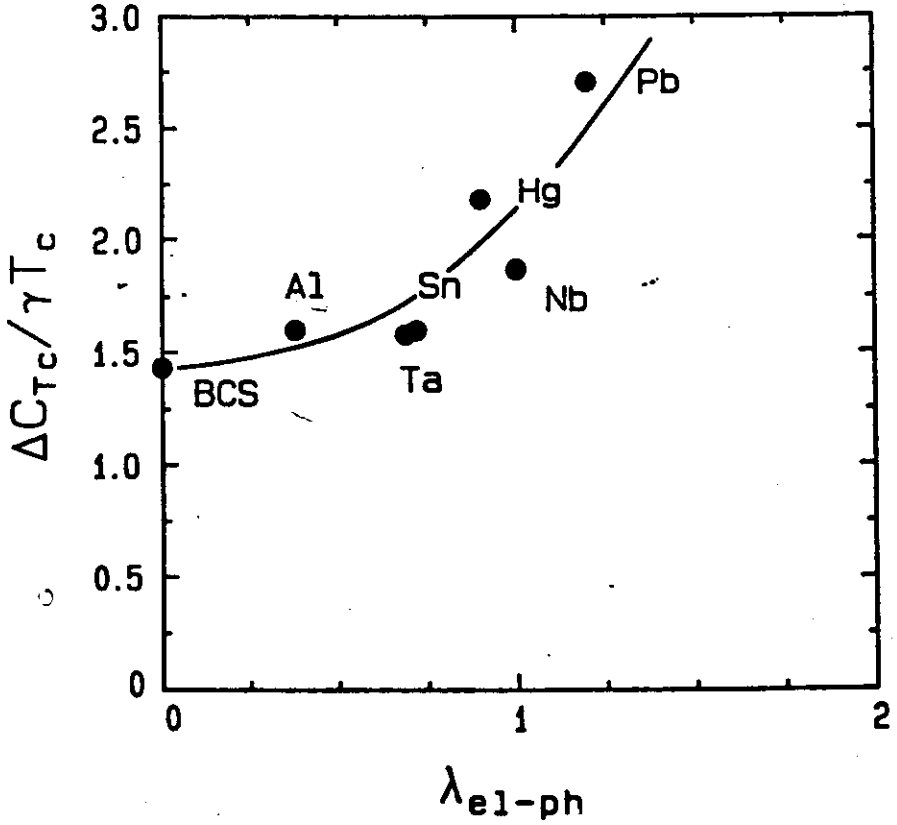

Magnetization finite-size effect

Clem and Kogan, Jpn. J. App. Phys., 26, 1161 (1987)
(also Schoenberg)

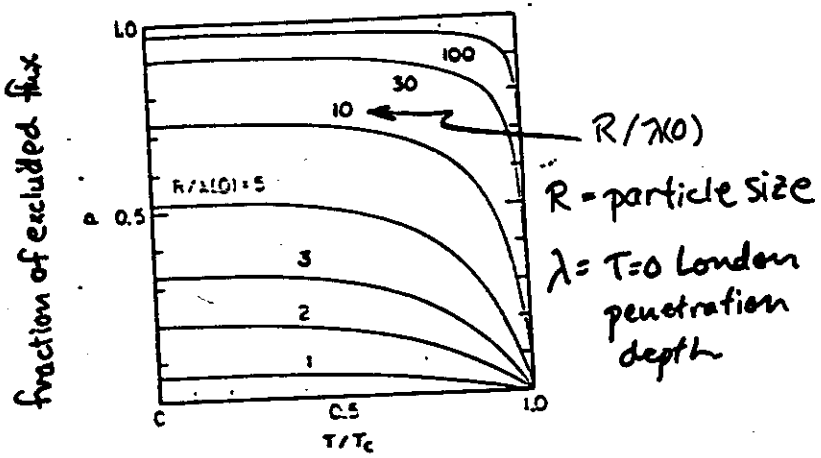

Fig. 1. $P(R/\lambda)$ versus T/T_c.

FINITE-SIZE effects cont.

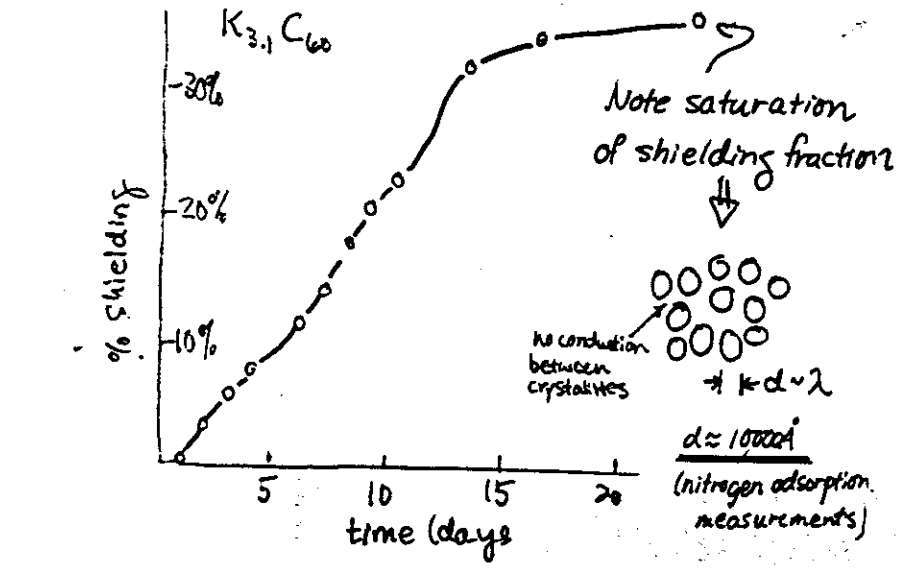

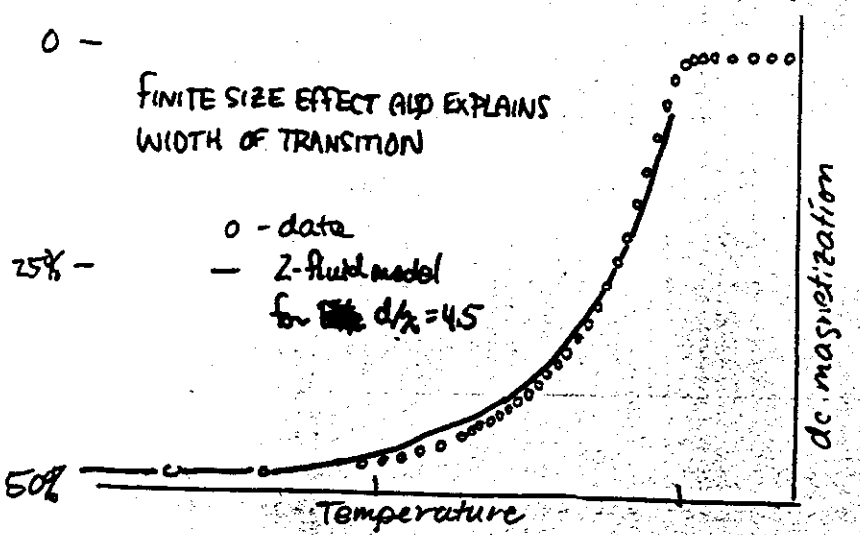

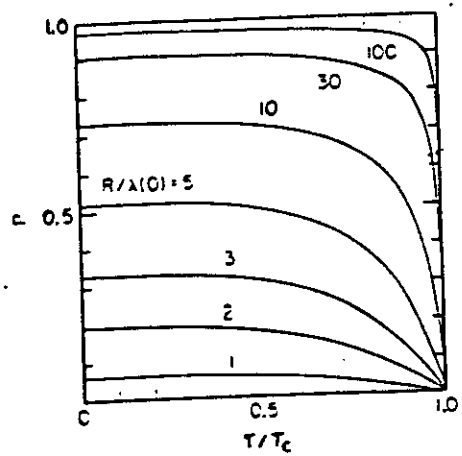

Fig. 1. $P(R/\lambda)$ versus T/T_c.

FINITE-SIZE effects

We know

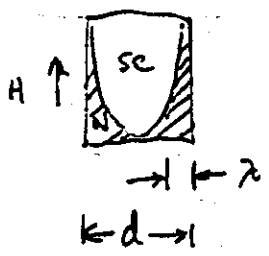

for small specimens,

$$|\bar{M}| < \frac{H}{4\pi}$$

Therefore, the critical fields are enhanced

$$\int_0^{H_c} M\,dH = F_S - F_N$$

e.g., for thin films. (London theory)

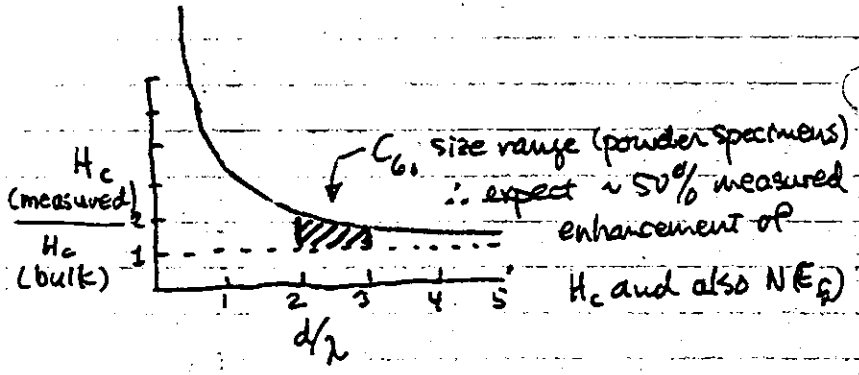

∴ Size-Corrected $N(E_f) \simeq 15 \pm 5$ states/ev C_{60}

Close to Band value ≈ 10 states/ev C_{60}
(correlation effects)

Specific Heat Jump in K_3C_{60}

High precision - with addendum

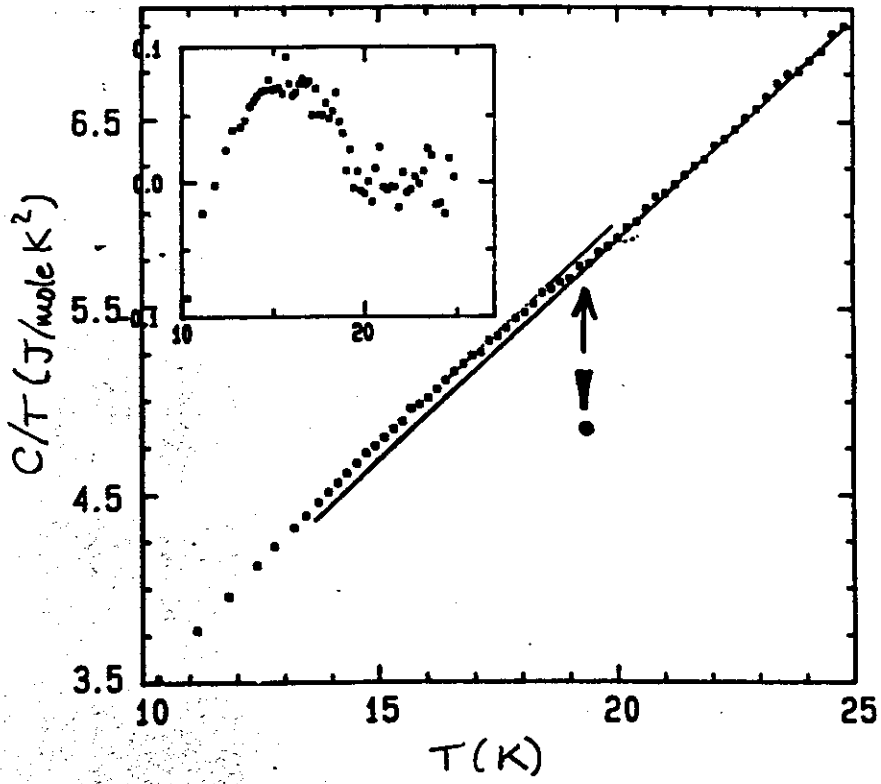

Specific heat jump at T_c - polycrystalline samples

Batlogg, Dynes Physica 126B (1984)

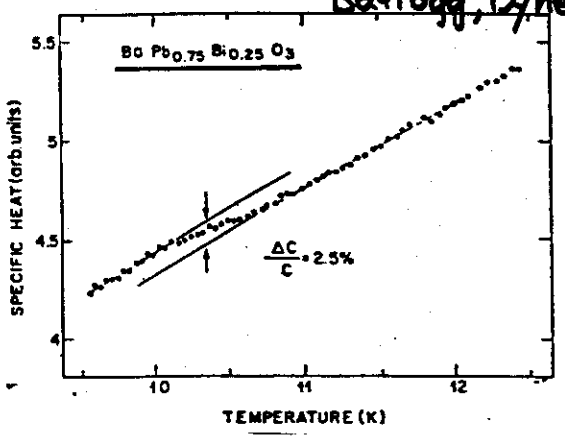

High resolution measurements of the specific heat. The small anomaly at T_c corresponds to a Sommerfeld constant γ of 1.5 ±0.2mJ/mole K².

Ramirez et al., PRB (1987)

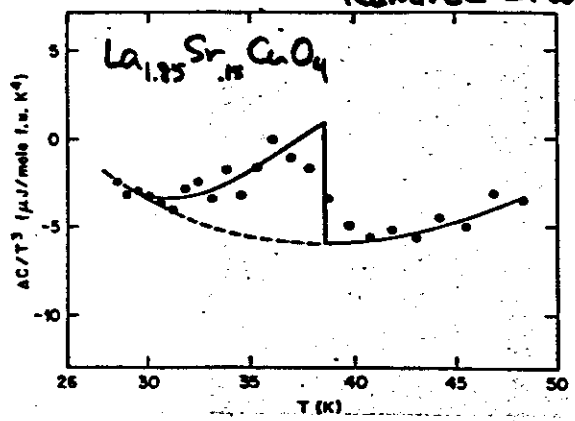

FIG. 4. The specific-heat difference ΔC between the measured values and the results of the fitting procedure as described in the text, in the vicinity of T_c. The curves shown here are guides to the eye and the jump at T_c is estimated to be 10 ± 2 mJ/mole f.u. K².

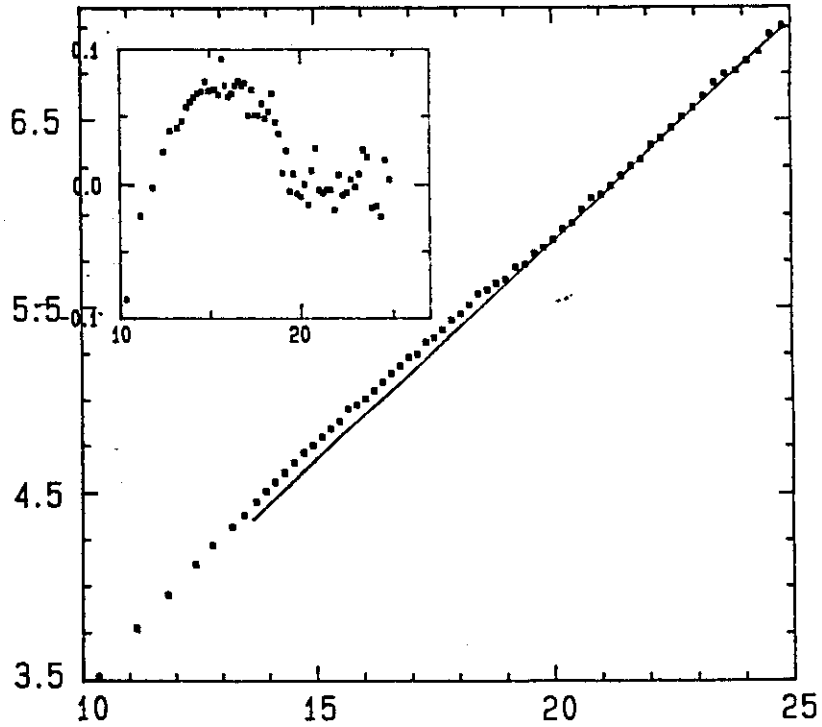

Specific Heat of K_3C_{60}

Ramirez, Rosseinsky, Murphy, Haddon
preprint, AT+T.

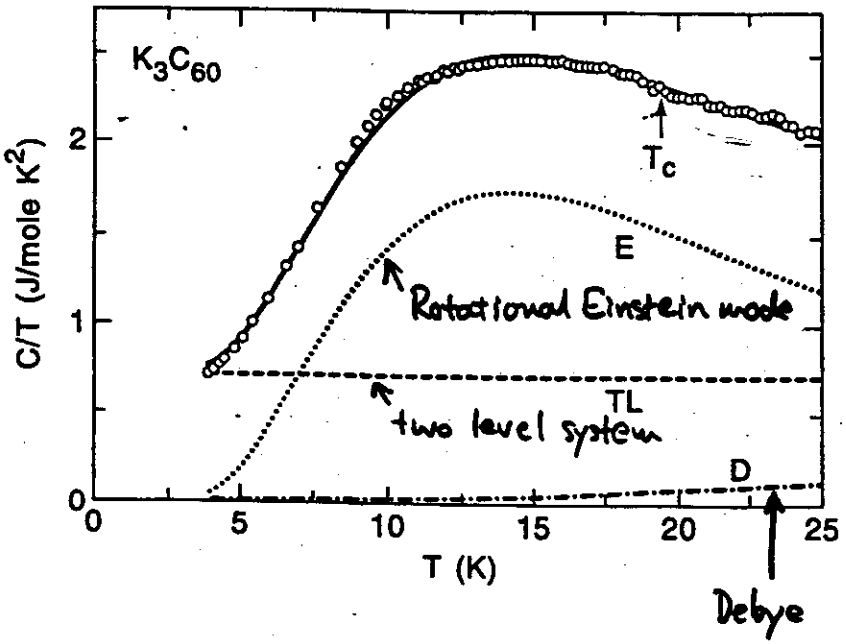

Fig. 2

Specific Heat of K_3C_{60}

Ramirez, Rosseinsky, Murphy, Haddon
preprint, AT+T

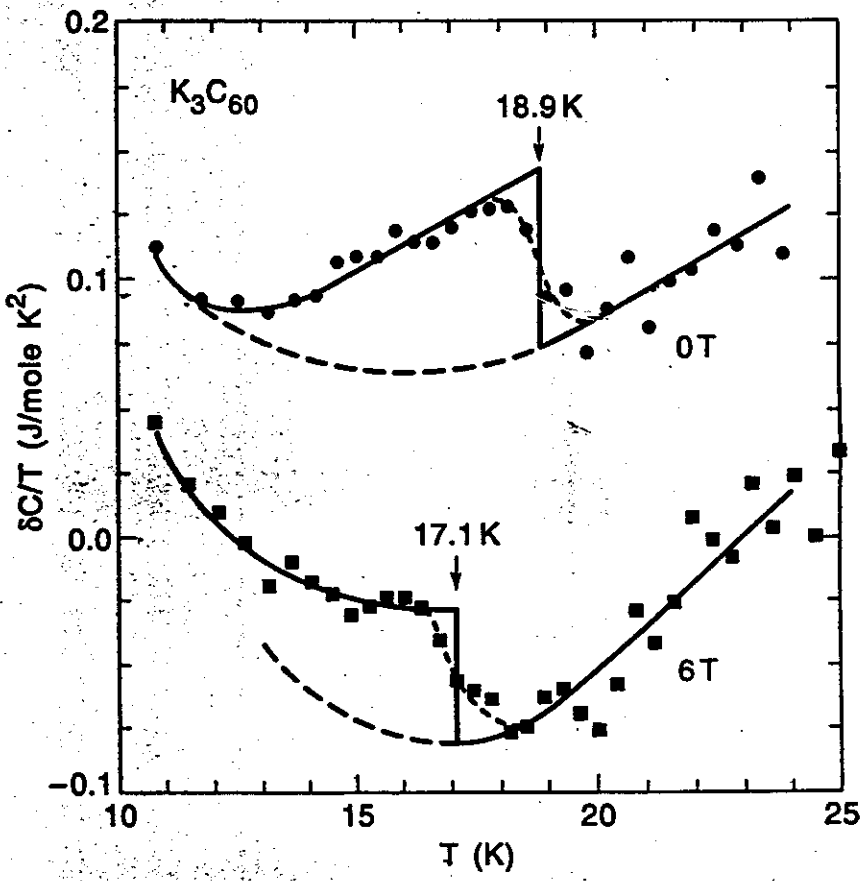

Fig. 3

Specific Heat Jump

$$\frac{\Delta C}{T_c} \approx 68 \pm 13 \ \text{mJ/molek}^2$$

$$\frac{\Delta C}{T_c} = 1.43(1 + 0.5\lambda_{ph}^2)\gamma$$

$$\gamma = \frac{2\pi^2 k_B^2}{3}(1 + \lambda_{ph} + \lambda_s) N_b$$

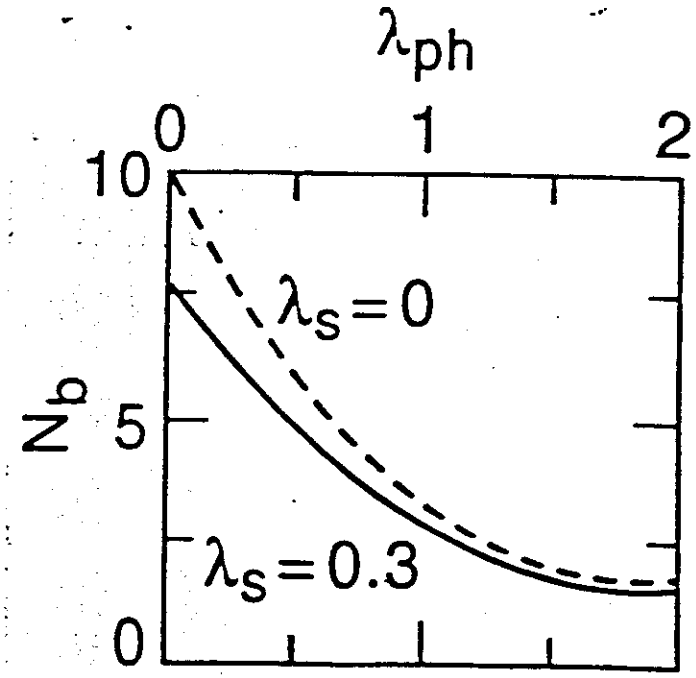

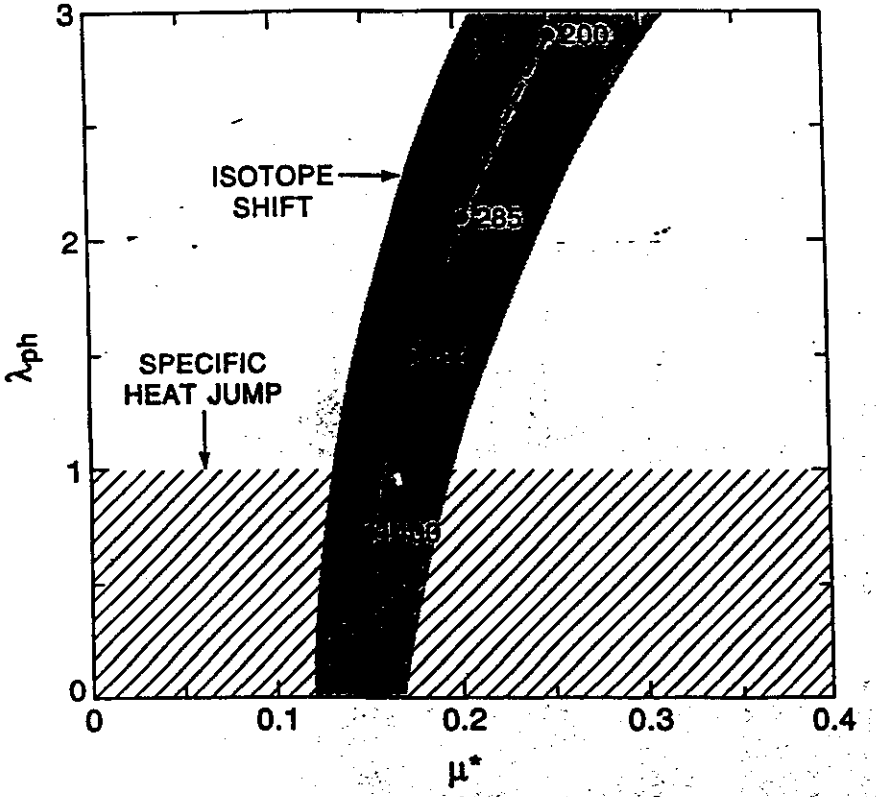

Fig. 4

Resistivity of single crystal K_3C_{60}

Xiang et al., Science, May 1992

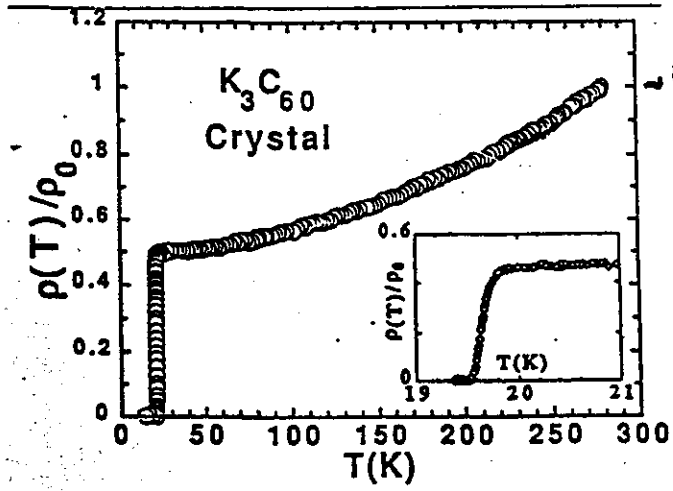

~ 5 mΩ·cm

- $\rho(T_c) \sim 2.5$ mΩ·cm $\approx \rho_{film}(T_c)$
- Possible diffusion barrier

Specific heat jump - continued.

Relationship between γ, $H'_{c2} = dH_{c2}/dT$

Clean limit

$$H'_{c2} = -1.5\times10^{-4}\,\gamma^2 T_c$$

H'_{c2}: 2 Tesla/K ; γ: ~ 38 mJ/mole K^2

? $\Leftrightarrow$ 0.2 Tesla/K

∴ Dirty limit (resistivity)

$$H'_{c2} = -0.89(1.5\times10^{-4}\gamma^2 T_c + 4.7\times10^{4}\,\gamma\rho)$$

Can derive $\rho = 0.5$ mΩ cm

$$l = v_F \tau = \frac{4800}{\rho} \approx 10\ \text{Å}$$ ← high orient. disorder

Explains low $\xi_{GL} = \sqrt{\xi_0 l} \approx 26$ Å for $\xi_0 \approx 120$ Å

agrees with TEM results

Infrared Reflectivity

Rotter et al, Nature, 355, 532 (1992)

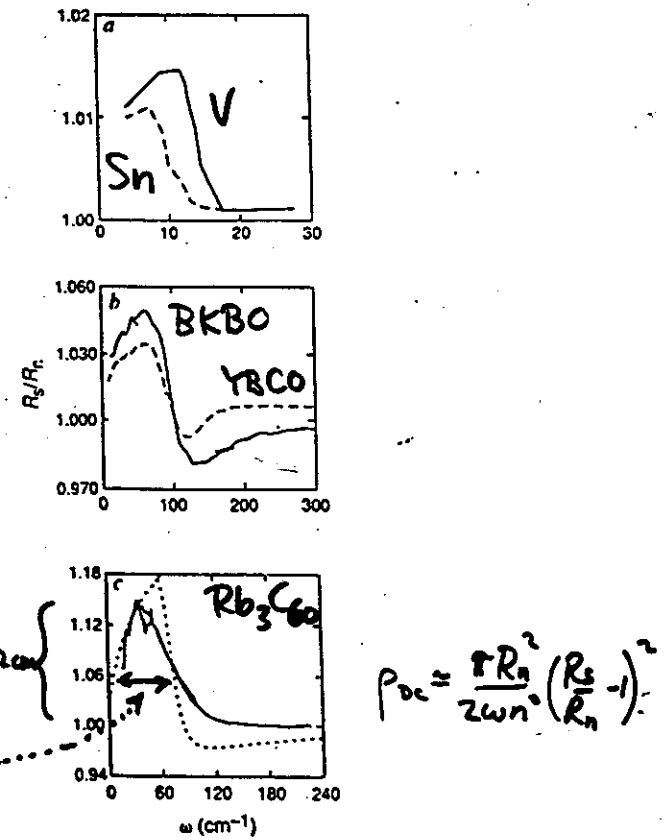

$\rho_{DC} \simeq 0.4$ mΩcm

$\frac{2\Delta}{kT_c} \simeq 3\text{-}5$

$$\rho_{DC} \simeq \frac{\pi R_n^2}{2\omega\lambda^2}\left(\frac{R_s}{R_n} - 1\right)^2$$

FIG. 1. a, The ratio of reflectivity in the superconducting state to that in the normal state measured in a cavity geometry is shown for vanadium (solid line) and tin (dashed). From these data, Richards and Tinkham[4] inferred energy gaps of $2\Delta \simeq 3.5kT_c$ for these superconductors. b, Similar reflectivity ratio from $Ba_{0.6}K_{0.4}BiO_3$, from which a gap $2\Delta \simeq 3.5kT_c$ was inferred[6]. The dashed curve is R_s/R_n for $YBa_2Cu_3O_7$ scaled on the frequency axis by 0.15 (ref. 12). c, Ratio of the superconducting (8 K) to normal (35 K) reflectivities for Rb_3C_{60}. The dotted curve shows for comparison a calculation[16] of R_s/R_n for a superconductor/sapphire interface for a moderately dirty superconductor ($\rho_{DC} \simeq 0.4$ mΩ cm) with $2\Delta \simeq 60$ cm^{-1}.

Fermi Surface of K_3C_{60}

Erwin and Pickett, Science 254, 842 (1991)

Fig. 2. First (blue) and second (yellow) sheets of the K_3C_{60} Fermi surface, each enclosing unoccupied states. Part of the second sheet is cut away to reveal the first sheet inside.

Fig. 3. Repeated-zone representation for the second sheet of the Fermi surface for K_3C_{60} which holds the charge carriers that become superconducting. The two symmetry-equivalent pieces (shown in different colors) are multiply connected along Cartesian axes although interconnecting.

DIMENSIONALITY AND SUPERCONDUCTIVITY

56

1-D	2-D	3-D
$A_2Mo_3X_3$	A_xMoS_2	AMo_6S_8
	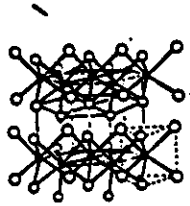	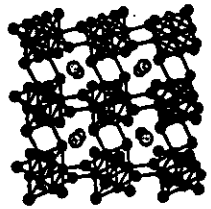
0 K	5 K	15 K
$(CH)_n$	Graphite (KC_8)	Rb_3C_{60}
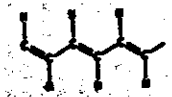	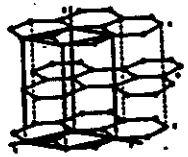	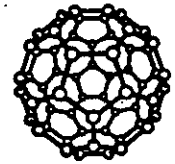
0 K	0.5 K	29.6 K
?	Cu-O planes	!
	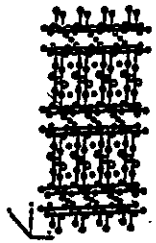	
?	125 K	!!

Specific Heat — Conclusion

- Magnitude of jump, $\Delta C/T_c$ is consistent with weak coupling, $\lambda \leq 1$, and probably not with the tunneling λ.

General Conclusions

- A_3C_{60} looks like a conventional phonon mediated superconductor, where $\langle\hat{\omega}\rangle$ is an intramolecular phonon frequency, $\approx$ 1500 K.
- Still have problem with Migdal's theorem.
- Unlikely to find $T_c > 33$ K by electron doping into the t_1 levels.
- Superconductivity in A_3C_{60} demonstrates the principle of working towards 3-dimensional molecular systems for higher T_c's.

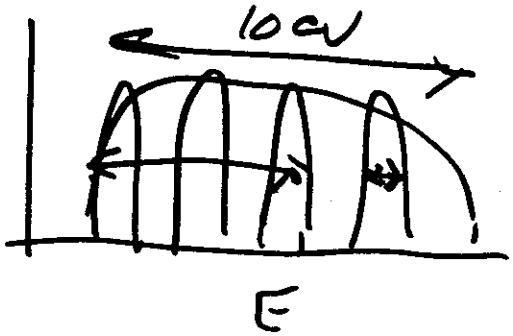

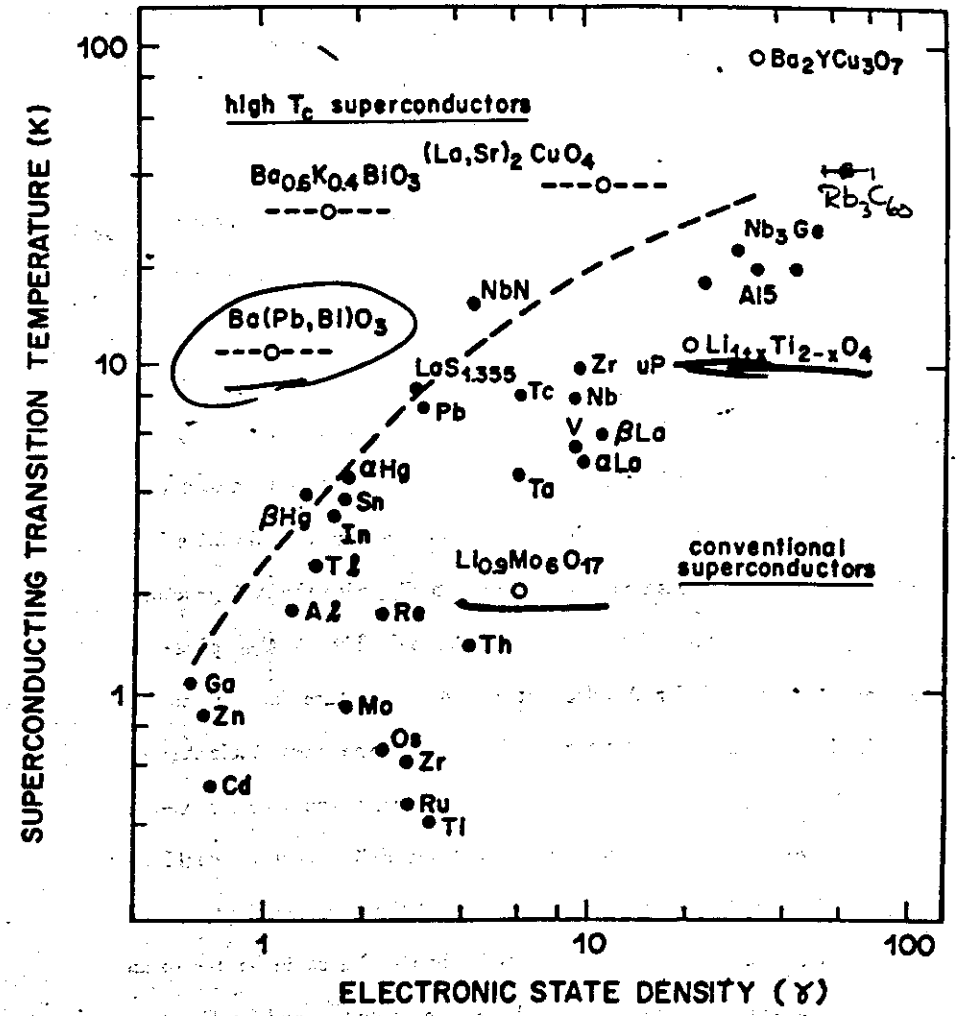

Progress of T_c with Time

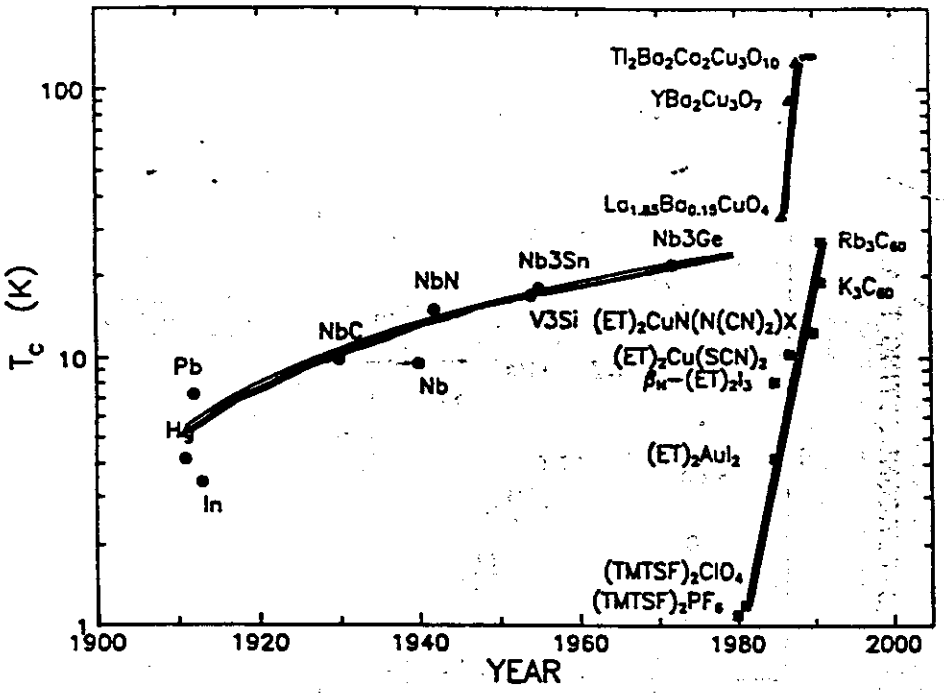

Jerome
Cond. Mat. News 1, (1992)

57

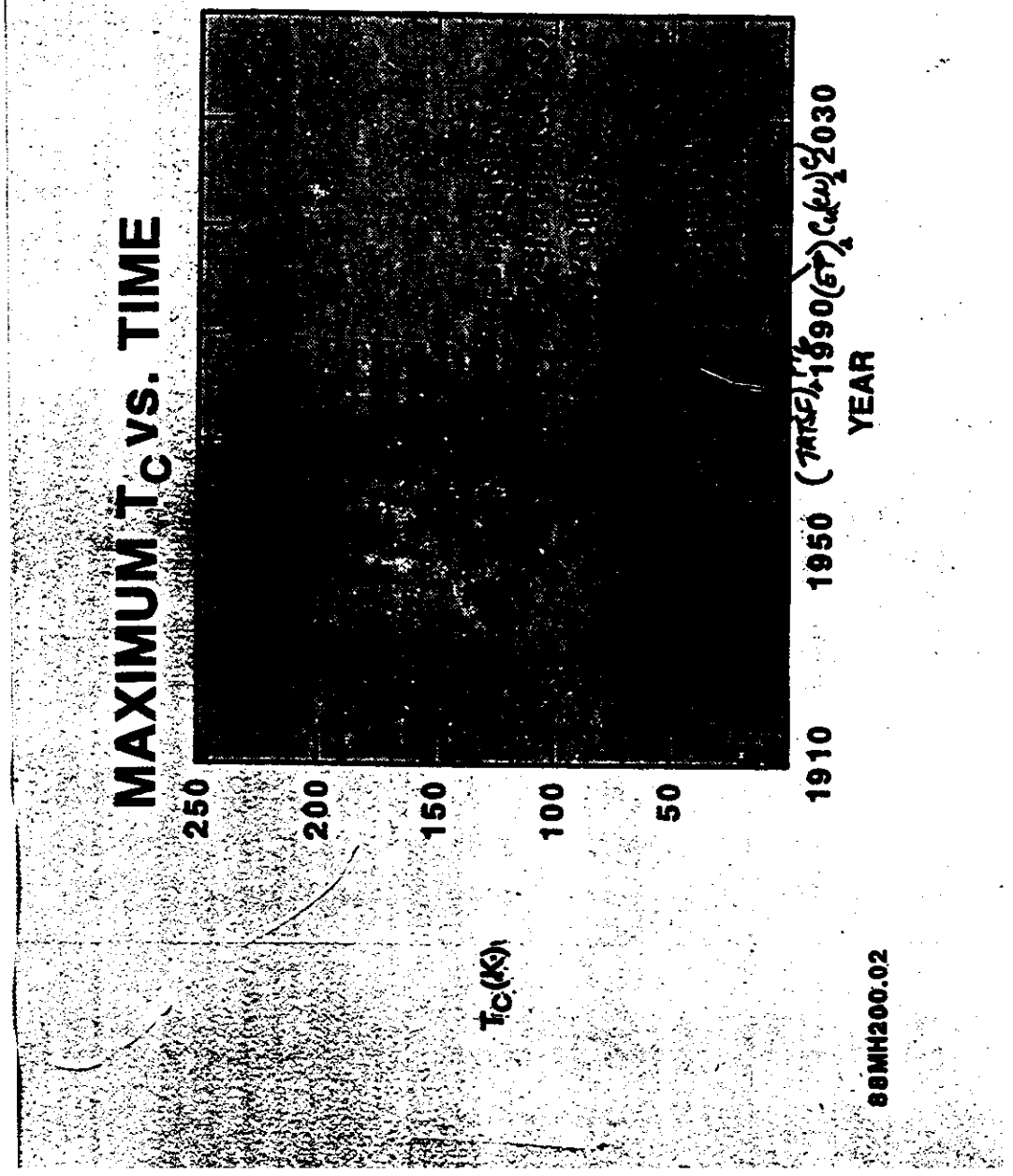

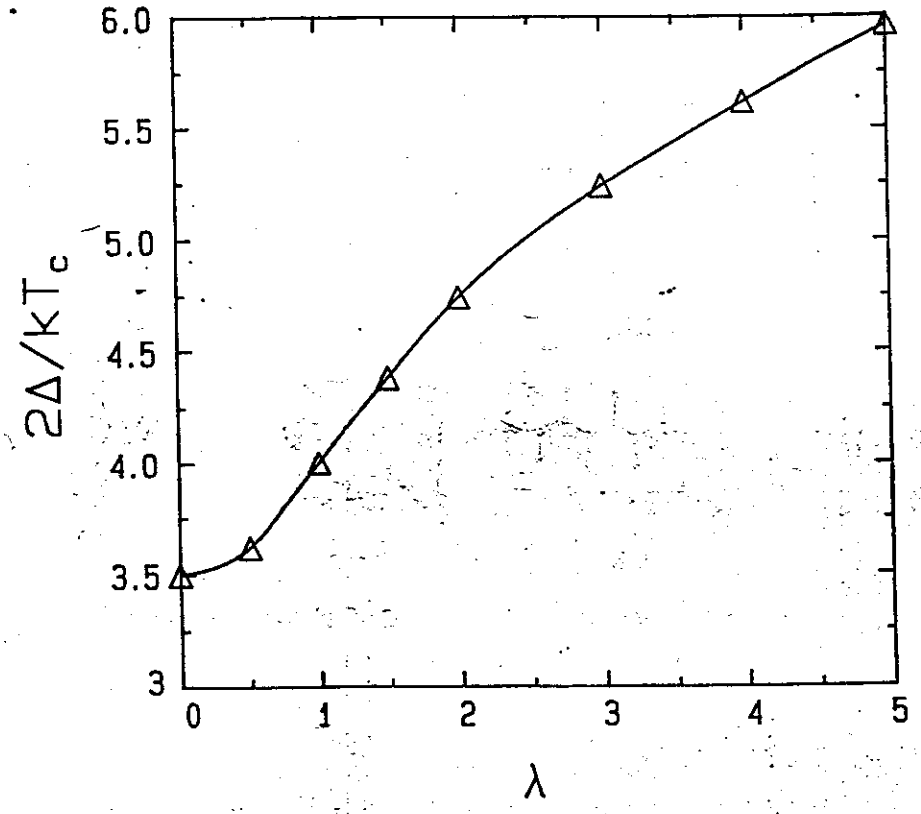

Density of States (cont.)

- Specific heat N_o consistent with band structure N_o.

- Susceptibility N_o magnitude also consistent, but change from K_3 to Rb_3 is twice too large.

- Can reconcile with Stoner enhancement, $N_{meas} = N_{bare}/(1 - IN_{bare})$. Need $I \approx 2$, for high energy phonons.

- If $\langle n \rangle$ is small, ≈ 200 K, however, then no enhancement.

Density of States A_3C_{60} - Summary

	N_{bare}	N_χ	N_γ
NMR	–	20	–
XPS	2	–	–
critical fields	–	–	13
Susceptib.	"4-5"	20	–
specific heat	"4-6"	–	"13"
LDA	6		

$$N_\chi = \frac{N_b}{1 - IN_b}$$

$$N_\gamma = N_b(1+\lambda_{ph})$$

Specific Heat Jump K_3C_{60}
(phonon background subtracted)

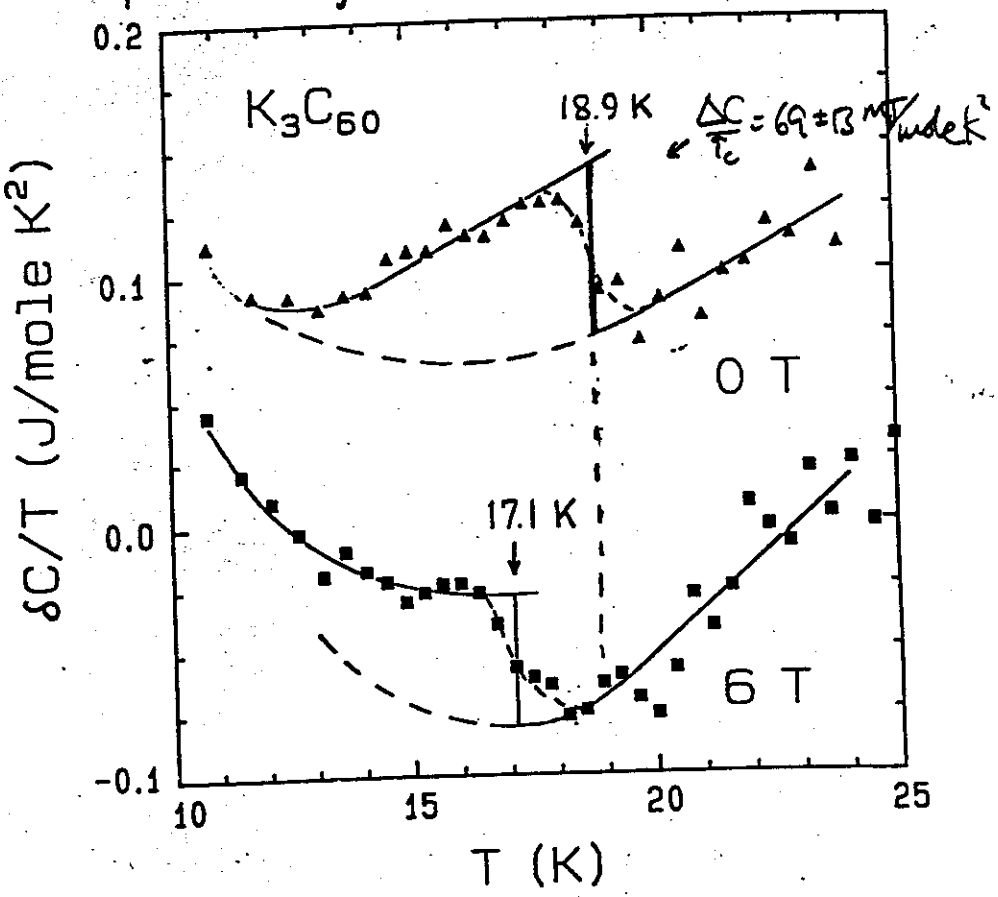

Fig. 2

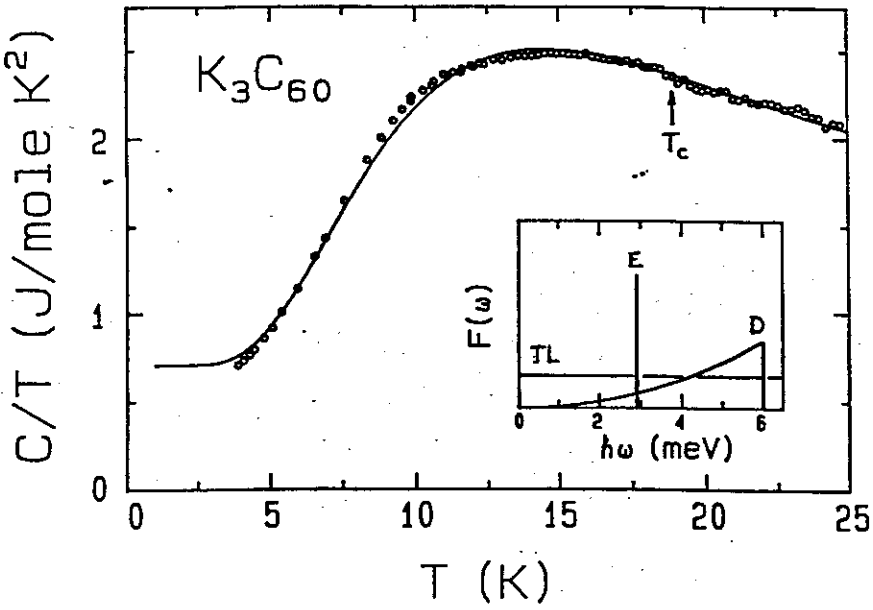

Fig. 1

Can large change in N_x be reconciled with the McMillan eqn.?

$\lambda = N_b V$ $\quad T_c = \frac{\hbar\omega}{1.2} \exp\left[\frac{-1.04(1+\lambda)}{\lambda - \mu^*(1+0.62\lambda)}\right]$

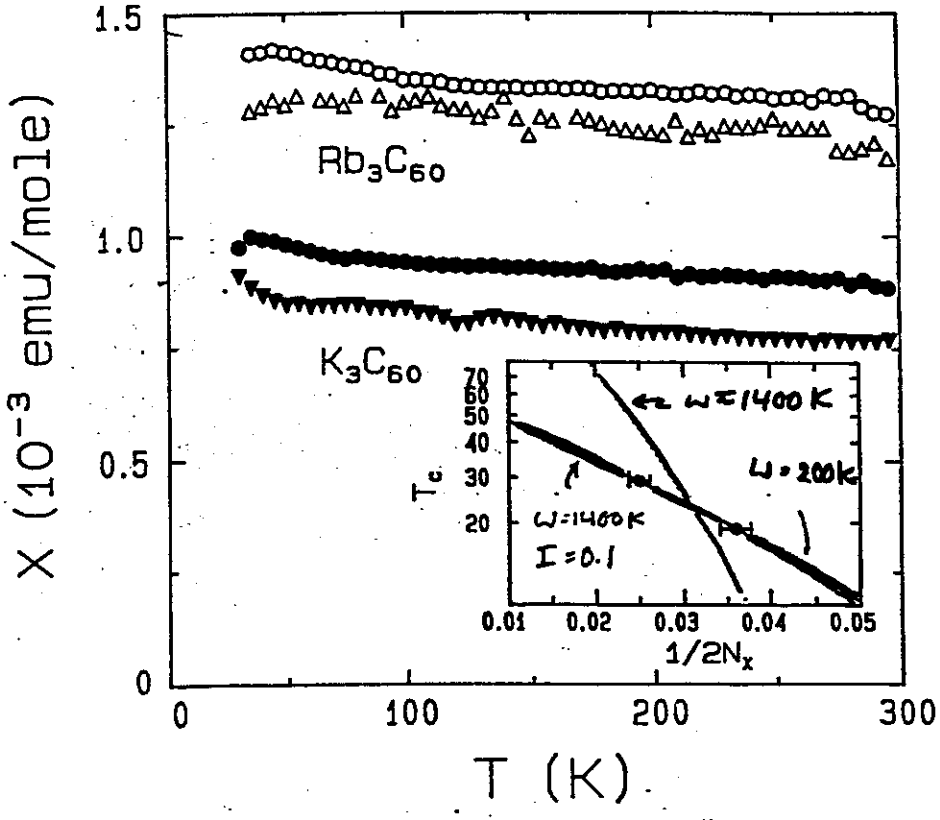

Fig. 3

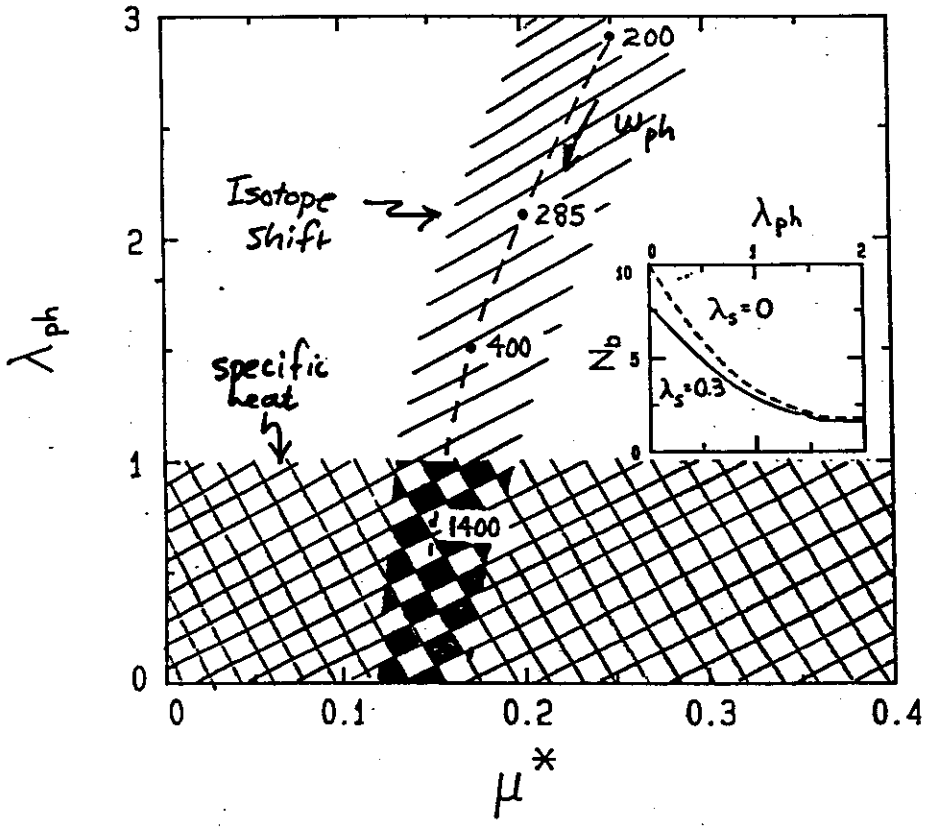

Fig. 4

Determination of $N^{\gamma}(\epsilon_F)$ through critical field measurements

Rutgers Relation

$$F_n - F_s = \frac{H_c^2(T)}{8\pi} \quad *$$

$$\Downarrow$$

$$\frac{\Delta C}{T_c} = \frac{(H_c')^2 V_{mol}}{4\pi}$$

assume BCS ($\Delta C/T_c = 1.43\,\gamma$)

$$N^{\gamma}(\epsilon_f) = \frac{3}{\pi^2 k_B^2} \frac{1}{1.43} \frac{V_{mol}}{4\pi} (H_c')^2$$

$$* \quad H_c^2 = \frac{H_{c1} H_{c2}}{\ln \kappa} \quad ; \quad \frac{H_{c1}}{H_{c2}} = \frac{\ln \kappa}{2\kappa^2}$$

Upper Critical Field, H_{c2}, determination

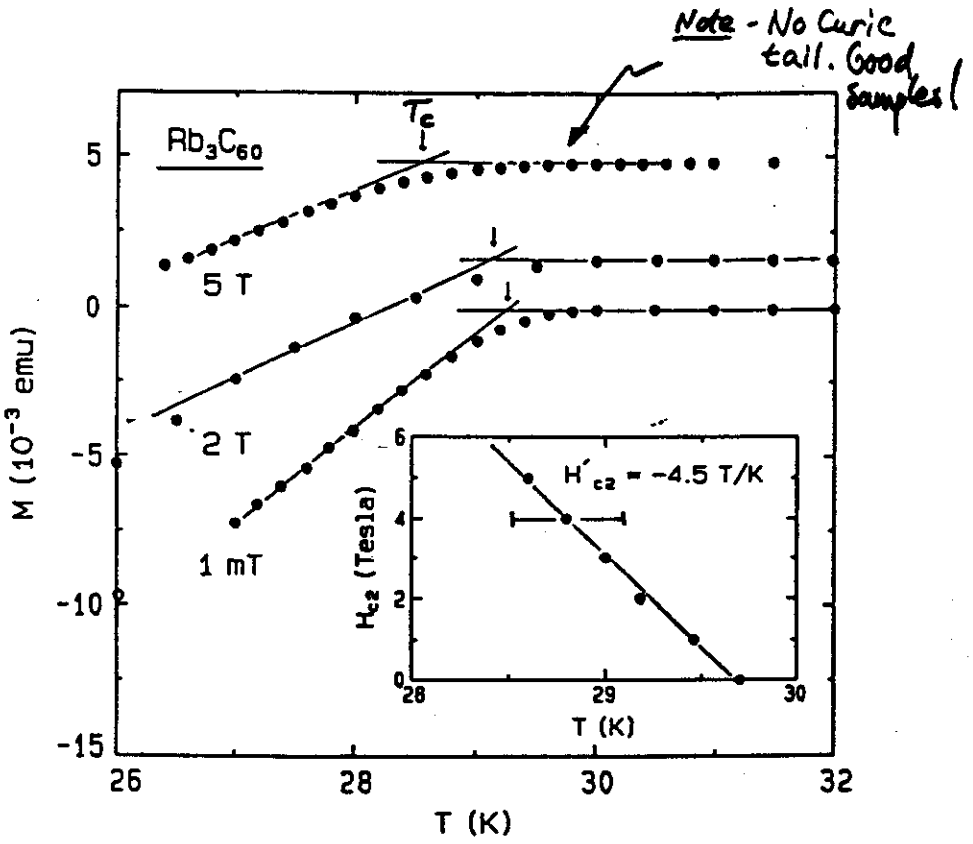

FIG. 3

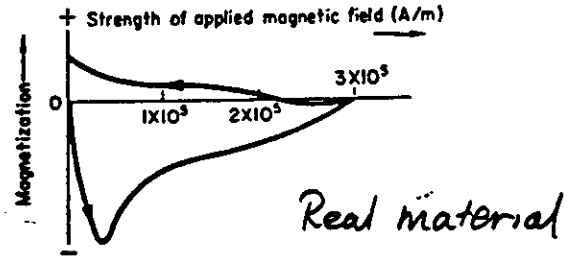

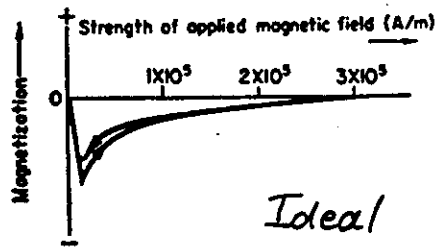

Lower Critical Field, H_{c1}, determination.

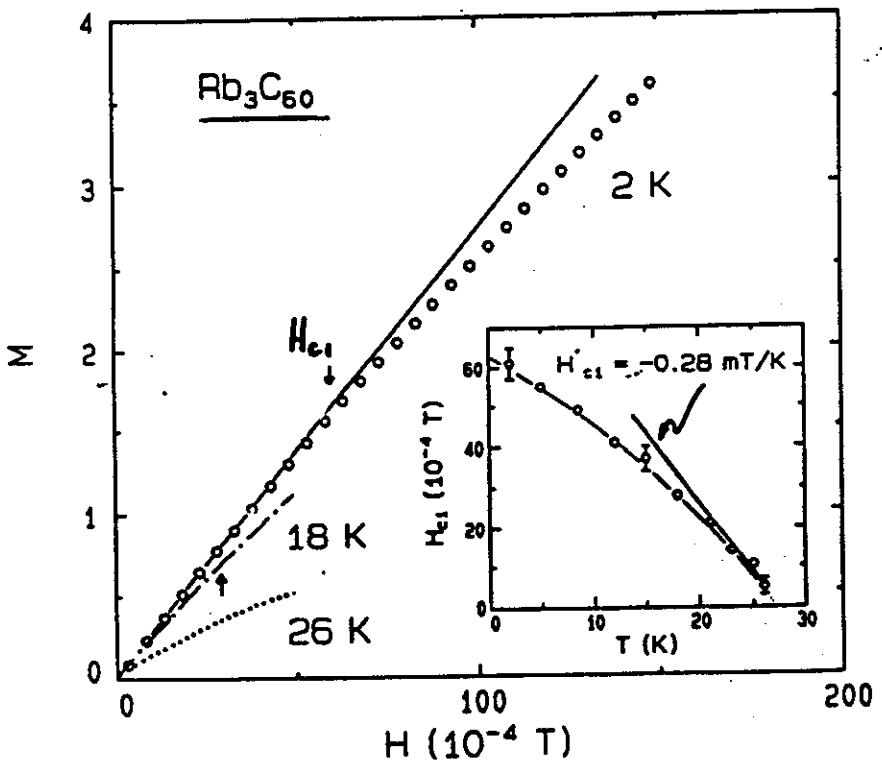

$$H_{c1} = \frac{\Phi_0}{4\pi\lambda^2} \ln\kappa \Rightarrow \lambda \sim 3500 \approx 900 \text{ Å}$$

In good agreement with μSR: $\lambda \simeq 4500$ Å

FIG. 2

μSR penetration depth Uemura et al.

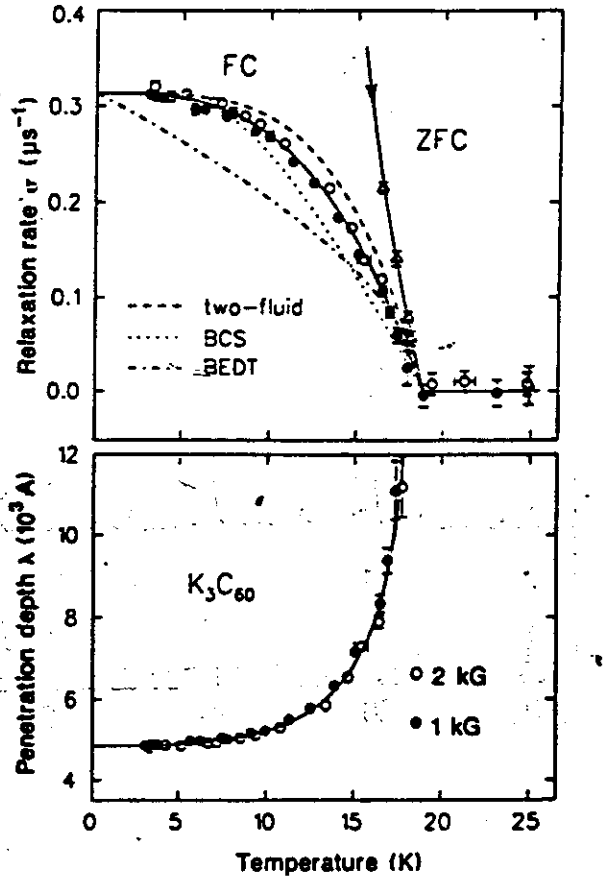

FIG. 2 a, Temperature dependence of the muon-spin-relaxation rate $\sigma(T)$ in K_3C_{60}. The solid line shows a fit to $\sigma(T) = [1-(T/T_c)^{3.2}]$ with $T_c = 18.9$ K. Also shown are curves expected for the two-fluid model, the BCS weak-coupling model and a recent μSR result in the BEDT system after normalizing by T_c. b, The magnetic field penetration depth λ in K_3C_{60} derived from $\sigma \propto \lambda^{-2}$.

Derived Superconducting Parameters Rb_3C_{60}

$K_{GL} \simeq 200$

$H_{c1} \simeq 60$ Oe $\quad / H'_{c1} = -0.28$ mT/K

$H_{c2} < 100$ T (clean limit) $/ H'_{c2} = -4.5$ T/K

$\gamma \simeq 60 \pm 10$ mJ/mole C_{60} K^2 (BCS)

$N^*(E_f) \geq 13 \pm 3$ States/eV C_{60} (Strong coupling will lower N^*)

If $\lambda (= NV) \sim 0.4$ then $N^* \simeq 6$